

Camila Schroeder

**EVALUATION OF BACTERIAL NANOCELLULOSE-
BIOGLASS COMPOSITES FOR HARD TISSUE ENGINEERING**

Dissertation submitted to the Graduate Program in Food Engineering at Federal University of Santa Catarina as part of the requirements for Master in Food Engineering.

Advisor: Prof. Dr. Bruno Augusto Mattar Carciofi

Co-advisor: Prof. Dr. Luismar Marques Porto.

Florianópolis

2018

Schroeder, Camila

Evaluation of bacterial nanocellulose-bioglass composite for hard tissue engineering / Camila Schroeder ; orientador, Bruno Augusto Mattar Carciofi, coorientador, Luissmar Marques Porto, 2018. 76 p.

Dissertação (mestrado) - Universidade Federal de Santa Catarina, Centro Tecnológico, Programa de Pós Graduação em Engenharia de Alimentos, Florianópolis, 2018.

Inclui referências.

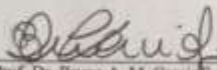
1. Engenharia de Alimentos. 2. Bacterial Nanocellulose. 3. Bioglass. 4. Tissue Engineering. 5. Bone Regeneration. I. Mattar Carciofi, Bruno Augusto. II. Marques Porto, Luissmar. III. Universidade Federal de Santa Catarina. Programa de Pós-Graduação em Engenharia de Alimentos. IV. Título.

**"EVALUATION OF BACTERIAL NANOCELLULOSE-
BIOGLASS COMPOSITE FOR HARD TISSUE
ENGINEERING"**

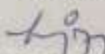
Por

Camila Schroeder

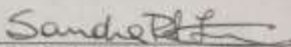
Dissertação julgada para obtenção do título de Mestre em Engenharia Alimentos, área de Concentração de Desenvolvimento de Processos da Indústria de Alimentos, e aprovada em sua forma final pelo Programa de Pós-graduação em Engenharia de Alimentos da Universidade Federal de Santa Catarina.



Prof. Dr. Bruno A. M. Carcioli
Orientador

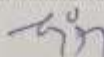


Prof. Dr. Luisimar Marques Porto
Coorientador



Prof. Dra. Sandra Regina Salvador Ferreira
Coordenadora

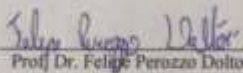
Banca Examinadora:



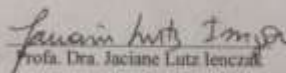
Prof. Dr. Luisimar Marques Porto



Dra. Fernanda Vieira Berti



Prof. Dr. Felipe Peruzzo Dolzot



Prof. Dra. Jaciane Lutz Ienczak

Florianópolis, 28 de setembro de 2018.

Dedico este trabalho aos meus pais,
Celso e Cleci, que não mediram
esforços para me apoiar em todas as
etapas da minha vida.
Amo muito vocês.

ACKNOWLEDGEMENTS

I would like to thank God for guiding me and giving me strength, ability and perseverance to continue. I want to use these opportunities and knowledge to make a better future.

I dedicate this work to my parents, Celso and Cleci, who have always encouraged me to be better. Thank you for all the support and effort to realize my dreams.

I would like to thank my co-advisor, Luismar Porto, for his guidance and enthusiasm about this research. I am grateful for the opportunity to be at Intelab and work on exclusive projects since 2012.

I would also like to thank my advisor, Bruno Carciofi, for his patience and advices.

I would like to offer my special thanks to Fernanda, who showed me this fascinating world; my passion for research and cells started by the experiences I had with you. Besides being a colleague, you are a wonderful friend.

My special thanks extend to Julia; her constructive recommendations mean so much to me. The seven years in the lab would not have been great without you and our friendship.

I would like to thank my colleagues-friends Karina, Guilherme, Emily and Maíra for their collaboration and companionship. The support of all Intelab group was crucial to my progress and success during these years.

The assistance of Felipe Daltoé and Gowsihan was very valuable. My scaffolds samples crossed the world for analyses and today produce good results.

I would like to thank the Central Laboratory technician, Leandro, for his help.

I am also grateful for the opportunity to participate in CsF program, was a great learning and professional development. I take this opportunity to express my gratitude to Professor Boccaccini, who devoted his time to listen and guide me at WW7 lab; to Professor Dachamir, who gave me the opportunity of the internship; and Judith Bortuzzo, who helped me with advices and several analyzes.

I would not forget to remind my Friends Ana, Cami, Lara and Nina for their support and for making my days happier.

I acknowledge the government's financial support throughout my study and research.

ABSTRACT

Bone losses due to degenerative diseases, traumas and dental defects have increased as a result of population aging, causing numerous limitations to the patients. The need to replace these damaged tissues and restore their physiological functions has increased the interest of researchers in developing new biomaterials. An ideal scaffold should have appropriate microstructures to facilitate cell attachment and proliferation, bear mechanical strength, be biodegradable and induce cell differentiation for tissue regeneration. The aim of this study is to produce and evaluate composites based on bacterial nanocellulose (BNC) and bioactive glass for hard tissue engineering. The scaffolds were synthesized by *ex situ* incorporation of Bioglass® (BG) particles into BNC matrices, where pre-produced polymer hydrogels were soaked in an aqueous solution of bioglass. The organic/inorganic composites are still novel in the literature, called BNC-BG, were characterized by Fourier transform infrared spectroscopy (FTIR) to understand the transformations occurred during scaffold synthesis and their morphology assessed by scanning electron microscopy (SEM). Furthermore, the composites were characterized as their mechanical properties and by Brunauer–Emmett–Teller (BET) method to evaluate their superficial area and pore volume. Bioglass® has an interesting trait when immersed in body fluid, a layer of hydroxyapatite (HA) forms on its surface, similar to inorganic component of bones. To assess this bioactivity, formation of apatite on their surface, BNC-BG composites were soaked in simulated body fluid and further analyzed by SEM micrographs and FTIR. Murine fibroblasts (L929) and preosteoblasts cells (MC3T3-E1) were seeded on the scaffolds and cultured *in vitro*. Results indicated that the composites have great potential for tissue regeneration, BNC-BG provided a major surface area for HA formation, improved mechanical strength and regulated the physiological activity of different cell lines; low BG concentration in BNC matrix favored proliferation of fibroblasts and larger, increased preosteoblastic metabolic activity. The developed three-dimensional BNC-BG scaffold suggests potential for hard tissue engineering and regeneration.

Keywords: Bacterial nanocellulose, bioactive glass, tissue engineering, bone regeneration

RESUMO

Avaliação de compósito nanocelulose bacteriana-biovidro para engenharia tecidual óssea

Perdas ósseas decorrentes de doenças degenerativas, traumas e defeitos dentais têm aumentado em função do envelhecimento populacional, causando inúmeras limitações aos pacientes. A necessidade de substituir esses tecidos danificados e restaurar sua funcionalidade fisiológica tem aumentado o interesse de pesquisadores em desenvolver novos biomateriais. Um scaffold ideal deve apresentar uma estrutura apropriada para a fixação e proliferação celular; suportar forças mecânicas; ser biodegradável; induzir a diferenciação celular e regeneração do tecido. O objetivo deste trabalho foi produzir um compósito à base de nanocelulose bacteriana (BNC) combinada com vidro bioativo. Os scaffolds foram sintetizados através da incorporação *ex situ* de partículas de Bioglass®(BG) à matriz polimérica da BNC. Os compósitos orgânico-inorgânico ainda inéditos na literatura, denominados BNC-BG, foram caracterizados por espectroscopia no infravermelho com transformada de Fourier (FTIR) para entender as transformações ocorridas durante sua síntese; e sua morfologia avaliada por microscopia eletrônica de varredura (MEV). Além disso, foram caracterizados quanto às suas propriedades mecânicas, área superficial e volume de poros. O Bioglass® tem uma característica interessante quando imerso em fluido corporal, uma camada de hidroxiapatita carbonatada se forma em sua superfície, semelhante ao componente inorgânico do osso. Para avaliar a bioatividade, formação de hidroxiapatita (HÁ) na superfície, os compósitos foram colocados em fluido corporal simulado e posteriormente analisados por MEV e FTIR. Células de fibroblastos murinas (L929) e pré-osteoblastos (MC3T3-E1) foram semeadas nos scaffolds e cultivadas *in vitro* durante sete dias. Os resultados indicaram que o compósito desenvolvido possui grande potencial para regeneração tecidual; forneceu uma maior área superficial para a formação de HA; melhorou a força mecânica e regulou a atividade fisiológica das diferentes linhagens celulares; em baixa concentração de BG na matriz de BNC, favoreceu a proliferação de fibroblastos e nas maiores, aumentou a atividade metabólica dos pré-osteoblastos. O scaffold BNC-BG desenvolvido apresenta enorme potencial para engenharia de tecidos e regeneração óssea.

Palavras-chave: Nanocelulose bacteriana, biovidro, engenharia de tecidos, regeneração óssea.

RESUMO EXPANDIDO

Avaliação de compósito nanocelulose bacteriana-biovidro para engenharia tecidual óssea

Introdução

Perdas ósseas decorrentes de doenças degenerativas, traumas e defeitos dentais têm aumentado em função do envelhecimento e aumento populacional, causando inúmeras limitações aos pacientes. A necessidade de substituir esses tecidos danificados e restaurar sua funcionalidade fisiológica tem aumentado o interesse de pesquisadores em desenvolver novos biomateriais. Um scaffold ideal deve apresentar uma estrutura apropriada para a fixação e proliferação celular; suportar forças mecânicas; ser biodegradável e biocompatível; induzir a diferenciação celular e regeneração do tecido. O grande potencial da nanocelulose bacteriana (BNC) tem sido explorado como um compósito para a engenharia de tecidos, devido à versatilidade dos componentes que podem ser adicionados a matriz de BNC; O vidro bioativo 45S5 Bioglass® apresenta biocompatibilidade, interação bioativa, propriedades osteogênicas e efeitos angiogênicos que guiam a regeneração tecidual.

Objetivos

O objetivo deste trabalho foi produzir um compósito à base de nanocelulose bacteriana (BNC) combinada com vidro bioativo . Os scaffolds foram sintetizados através da incorporação *ex situ* de partículas de Bioglass®(BG) à matriz polimérica da BNC em diferentes soluções; caracterizados segundo seu desempenho mecânico, cinética e distribuição de incorporação, interação dos componentes; e, avaliada a citotoxicidade *in vitro* dos compósitos de BNC-BG.

Metodologia

Os compósitos orgânico-inorgânico ainda inéditos na literatura, denominados BNC-BG, foram caracterizados por espectroscopia no infravermelho com transformada de Fourier (FTIR) para entender as transformações ocorridas durante sua síntese; e sua morfologia avaliada por microscopia eletrônica de varredura (MEV). Além disso, foram caracterizados quanto às suas propriedades mecânicas, área superficial e volume de poros. O Bioglass® tem uma característica interessante quando imerso em fluido corporal, uma camada de hidroxapatita carbonatada se forma em sua superfície, semelhante ao componente

inorgânico do osso. Para avaliar a bioatividade, formação de hidroxiapatita (HA) na superfície, os compósitos foram colocados em fluido corporal simulado e posteriormente analisados por MEV e FTIR. Células de fibroblastos murinas (L929) e pré-osteoblastos (MC3T3-E1) foram semeadas nos scaffolds e cultivadas *in vitro* para avaliar a atividade metabólica das células em contato com o material, assim como analisar, segundo a ISO 10993-5, a citotoxicidade pelo método colorimétrico de MTS.

Resultados e Discussão

Os resultados indicaram que o compósito desenvolvido possui grande potencial para regeneração tecidual. A síntese em solução contendo água proporcionou a melhor incorporação, onde partículas de BG foram homogeneamente integradas entre as nanofibras do polímero BNC; forneceu uma maior área superficial para a formação de HA; melhorou a força mecânica e regulou a atividade fisiológica das diferentes linhagens celulares. Baixa concentração de BG na matriz de BNC, favoreceu a proliferação de fibroblastos e nas maiores, aumentou a atividade metabólica dos pré-osteoblastos, apresentando biocompatibilidade e potencial do biomaterial para regeneração de tecidos duros. O presente estudo concentrou-se no desenvolvimento de um material compósito BNC-BG para engenharia de tecidos duros; no entanto, mesmo que ocorra inibição de células fibroblásticas, esse fato pode ser benéfico, pois, se houver crescimento excessivo de fibroblastos, pode inibir o crescimento de outros tipos celulares, como células endoteliais ou osteoblastos, impossibilitando o uso desse material em outros tecidos.

Considerações Finais

Partículas de vidro bioativas encapsuladas pela matriz de BNC podem efetivamente regular a atividade fisiológica de diferentes linhas celulares. A taxa de incorporação de BG pode ser prevista, indicando a possibilidade de projetar compostos com concentração específica que as células específicas necessitam. Isto implica que os hidrogéis BNC-Bioglass® podem distinguir notavelmente seu uso na engenharia de tecidos moles e tecidos duros e sugere potencial uso avançado como biomaterial para a regeneração óssea. O scaffold BNC-BG desenvolvido apresenta enorme potencial para engenharia de tecidos e regeneração óssea.

Palavras-chave: Nanocelulose bacteriana, biovidro, engenharia de tecidos, regeneração óssea..

LIST OF FIGURES

Figure 1 - Representative scheme of bacterial nanocellulose network. In detail, hydroxyl groups of nanofibers are showed	26
Figure 2 - Bacterial nanocellulose hydrogel (a) at air-liquid interface produced in static condition and (b) after purification.	27
Figure 3 - – Compositional dependence of bone bonding regions for bioactive glasses. The regions represent: (a)Class B glasses; (b) and (c) non-bonding glasses,where reactivity are too low and too high, respectively; (d) non glass forming; and (e) Class A glasses.....	30
Figure 4 – Schematic illustration of HCA formation from a bioactive glass exposed to SBF.....	31
Figure 5 –Schematic representation of the tissue engineering procedure, detailing for implants in articular cartilage tissue.	34
Figure 6 - Diagram representing the structure of this work and the experiments performed.....	37
Figure 7 – <i>Ex situ</i> incorporation of BG particles onto the unmodified BNC hydrogels.	38
Figure 8 - Samples fixation for tensile strength test.	40
Figure 9 – Schematic experimental set-up on the Diamond-Manchester Branchline and typical results.....	41
Figure 10 – Photographs of a) BNC hydrogel before incorporation and BNC-Bioglass® after 1 day soaked in b) water, c) 25%EtOH and d) 50%EtOH solutions with BG particles (1% w/v).	45
Figure 11 - Photography showing the detailed BNC-BG composite; synthesized after 1 day in water soaking solution with 1% w/v of BG particles.	46
Figure 12 – SEM images from (a) pure BNC membrane, and (b) BG particles and their random sizes.	46
Figure 13 –SEM micrographs of (a) unmodified BNC fibers; (b), (c) and (d) BNC-bioactive glass composites after 24 hours soaked in water with 0; 25 and 50% v/v of ethanol, respectively. Homogeneous distribution of BG particles covers the BNC surface in BNC-BG (b) and BNC-BG-25%EtOH (c).	47
Figure 14 - (a) Cross section of the BNC-BG composite. In detail (b), BG particle ingrained between the nanofibers.....	48
Figure 15 – FTIR results of (a) unmodified BNC (control) and BNC+BG composites soaked in (b) water; (c) 25% v/v EtOH solution and (d) 50% v/v EtOH solution.....	49

Figure 16 – 3D volume rendering of the BNC-BG hydrogel, composed of cross-sectional stacked images. Homogeneous dispersion of the particles inside the membrane is observed.....	50
Figure 17 SEM images of BNC-BG after 1 day in simulated body fluid. Micrographs (a), (b),(c), and (d) showed magnification of 1,000x, 2,000x, 5,000x and 10,000, respectively.....	51
Figure 18 – Results of EDX analysis for BNC-BG composites after 7 days in SBF showing elemental surface mapping of the HA layer.	51
Figure 19 SEM images of BG particles after (a), (b) 1day in SBF, magnification of 30,000x and 80,000x, respectively; and (c), (d) 7 days in SBF using magnification of 30,000x and 80,000x, respectively. A denser HA layer can be seen after a longer time.....	52
Figure 20 SEM micrograph of a detailed HA crystal on the nanofibers of BNC (80,000 × magnification).	52
Figure 21 – FTIR spectra of BNC-BG synthesized in water solution, before and after immersion in SBF.	53
Figure 22 – SEM images showing surface morphologies and pores, for: control BNC; and BNC-BG composites.....	54
Figure 23 – Characteristic stress–strain curves from tensile test for BNC and BNC-BG scaffolds (a). Average tensile strength values of each set of samples with elongation percentage are summarized (b)....	56
Figure 24 – Fracture strength images for BNC and BNC-BG obtained for loading in tension.....	57
Figure 25 BNC-BG incorporation profile when soaked in water solution with BG 1 % (w/v).	58
Figure 26 Cell proliferation assays on BNC scaffolds with or without bioactive glass additions.	59
Figure 27 – L929 cells after 7 days cultured in BNC (a) and BNC-BG (b) hydrogels. Live cells (green) are distinguished from dead cells (red).	60
Figure 28 Cell proliferation assays on pure BNC scaffolds and BNC-BG with different contents of BG particles.	62
Figure 29 – Metabolic activity of osteoblasts cells.	63

LIST OF ABBREVIATIONS

- 3D - Three dimensions
- BET - Brunauer–Emmett–Teller
- BG - Bioglass 45S5
- BNC - Bacterial nanocellulose
- BTE - Bone Tissue Engineering
- DMEM - Dulbecco's modified Eagles Medium
- EDS - Energy Dispersive X-ray Spectroscopy
- EMC - Extracellular Matrix
- FBS - Fetal Bovine Serum
- FDA - Food and Drug Administration
- FTIR - Fourier-transform infrared spectroscopy
- HA - Hydroxyapatite
- HCA - Hydroxyl carbonate apatite
- L929 - Murine fibroblasts cell line
- MC3T3-E1 - Murine preosteoblasts cell line
- MTS - [3-(4,5-dimethyliazol-2-il)-5-(3-carboximetoxifenil)-2-(4-sulfofenil)-2H-tetrazólio]
- OD - Optical density
- OMS - Organização Mundial da Saúde
- PBS - Phosphate buffered saline
- RPM - Rounds per minute
- SBF - Simulated Body Fluid
- scCO₂ - Supercritical carbon dioxide
- SEM - Scanning Electron Microscope
- TE - Tissue Engineering

LIST OF CONTENTS

1	INTRODUCTION.....	23
1.1	OBJECTIVES.....	24
1.1.1	General objective	24
1.1.2	Specific objectives	24
2	LITERATURE REVIEW.....	25
2.1	BIOMATERIALS AND THE IDEAL SCAFFOLD	25
2.2	BACTERIAL NANOCELLULOSE HYDROGELS AS A MATRIX FOR TISSUE ENGINEERING APPLICATIONS.....	26
2.3	BIOACTIVE GLASS SCAFFOLDS.....	29
2.4	COMPOSITES FOR BIOLOGICAL APPLICATIONS	33
2.5	TISSUE ENGINEERING.....	33
2.5.1	Bone tissue engineering	35
3	MATERIALS AND METHODS	37
3.1	DEVELOPMENT OF BNC-BG POLYMERIC COMPOSITES	37
3.1.1	BNC hydrogel synthesis	37
3.1.2	<i>Ex situ</i> incorporation of Bioglass® into BNC hydrogels	38
3.2	CHARACTERIZATION OF BNC-BG COMPOSITES	39
3.2.1	<i>In vitro</i> bioactivity of BNC-BG composites.....	39
3.2.2	Scanning Electron Microscopy (SEM) with Energy Dispersive Spectroscopy (EDS)	39
3.2.3	Chemical characterization of BNC-BG composites.....	39
3.2.4	Characterization of the surface area and pore volume of BNC and BNC–BG hydrogels	40
3.2.5	Mechanical properties measurement	40
3.2.6	Synchrotron Radiation.....	40
3.3	IN VITRO ASSAY.....	41
3.3.1	Cell culture	42
3.3.2	Viability and proliferation of fibroblast cells.....	42

3.3.3	Metabolic activity of MC3T3-E1.....	43
3.3.4	Statistical analysis.....	43
4	RESULTS AND DISCUSSION	45
4.1	PRODUCTION BNC-BG COMPOSITES	45
4.2	CHARACTERIZATION OF BNC-BG COMPOSITES.....	46
4.2.1	Morphological behavior	46
4.2.2	Fourier transforms infrared spectroscopy	48
4.2.3	Synchrotron X-ray tomography.....	49
4.2.4	<i>In vitro</i> bioactivity of BNC-BG composites	50
4.2.5	Characterization of the surface area and pore volume of BNC and BNC–BG hydrogels.....	53
4.2.6	Incorporation Kinetics of Bioglass [®] into BNC matrix	57
4.3	IN VITRO TESTS.....	58
4.3.1	Proliferation of L929 fibroblasts.....	58
4.3.2	Metabolic activity of MC3T3-E1 on BNC and BNC-BG hydrogels.....	62
5	CONCLUSIONS	65
5.1	SUGGESTED FUTURE WORKS.....	65
	REFERÊNCIAS	67

1 INTRODUCTION

The world's population is projected to increase more than one billion people over the next years, reaching 8.6 billions in 2030. Globally, population aged over 60 is growing faster than all younger groups, as published in World Population Prospects (2017); consequently, these citizens are more prone to suffer from diseases inherent to aging, or to be affected by traumas. In order to improve the quality of life, new approaches should focus on solutions to these issues as fresh priorities (HENCH, 1998; WEN et al., 2018).

The need to substitute damaged tissues and to restore their physiological functionality has always been the driving force for researchers to discover and design new biomaterials (BAINO; HAMZEHLU; KARGOZAR, 2018). Tissue engineering has been considered a promising biomedical technology that aims the repair and regeneration of flawed tissues (LANGER; VACANTI, 1993).

Biomaterials are in increasing relevance for tissue engineering approaches, displaying the ability to induce or stimulate tissue regeneration, where a series of multifunctional scaffolds can play these functions. In the field of bone tissue engineering, composite biomaterials based on polymer and bioactive glasses are specially being investigated.

In this context, the Biological Engineering Integrated Laboratories (LIEB) from Federal University of Santa Catarina, previously known as Integrated Technologies Laboratory (InteLab), develop innovative processes and products for chemical, biotechnological and medical applications. The great potential of bacterial nanocellulose (BNC) has been explored by multidisciplinary researchers, who have obtained significant results for several tissue engineering areas; BNC scaffolds for drug release system (CACICEDO et al., 2016), artificial blood vessels (COLLA, 2014; BERTI et al., 2016), epithelial tissue repair (GODINHO et al., 2016; PITELLA, 2017), as a matrix to modulate cell proliferation (BERTI et al., 2013; REIS et al., 2017). The potential of this polymer as a composite is growing because of the versatility of components that can be added to BNC. Different approaches that combine bioactive particles, functional groups and antimicrobial molecules can further enhance BNC properties and functions (PERTILE et al., 2012; JOZALA et al., 2016).

The Institute for Biomaterials at the Department of Materials Science and Engineering, from the University of Erlangen-Nuremberg conducts researches in a range of bioactive materials for medical

implants, tissue engineering and drug delivery. Current projects, in the field of glasses, ceramics and composites, are focused on bone, cartilage and cardiac tissue regeneration. A silicate glass, 45S5 Bioglass®, has been intensively studied for this purpose, because of its biocompatibility, bioactive interaction, osteogenic properties, angiogenic effects that guide tissue regeneration (LI et al., 2014; ROMEIS et al., 2015; BALASUBRAMANIAN et al., 2018). The institute led by Professor Aldo R. Boccaccini provides international leadership in the biomaterials field, especially with Bioglass® works.

Due to the properties of the BNC matrix and the promising characteristics of 45S5 bioactive glass, a composite was developed in partnership between the laboratories, where bioglass particles were incorporated into BNC hydrogels. The present work presents the synthesis and evaluation of BNC-BG composites for tissue engineering applications.

1.1 OBJECTIVES

1.1.1 General objective

Development of bacterial nanocellulose-bioactive glass scaffolds for potential application in hard tissue engineering.

1.1.2 Specific objectives

Synthesize a composite based on bacterial nanocellulose and Bioglass® through *ex situ* incorporation into the polymer matrix by different bulk solutions;

Characterize the BNC-BG composites:

- Distribution of BG particles between BNC fibers;
- Interaction among BNC and BG components;
- Incorporation kinetics of BG particles into the hydrogels;
- Mechanical performance of the composite;

Evaluate the biological response of fibroblasts and osteoblasts cells and assess the *in vitro* cytotoxicity of BNC-BG composites.

2 LITERATURE REVIEW

2.1 BIOMATERIALS AND THE IDEAL SCAFFOLD

Biomaterials are natural or synthetic substances, projected to interact with biological systems, usually as part of medical devices (KARAGEORGIU; KAPLAN, 2005). As a science, biomaterials play an important role in medical applications; integrate fields as biology, chemistry, material science and influences from tissue engineering (TE).

Non-biological materials have been used as surgical implants for a long time, especially in substitution of bone parts in the human body (OHGUSHI et al., 2000). However, in the course of years, the advances in this science have developed novel materials. First generation of biomedical goods had the purpose to be as bioinert as possible, with minimal immune response to the recipient; then, in second generation, the emphasis shifted to produce active biomaterials, able to induce controlled biological reactions and improve the biomaterial-body interface. More recently, the third-generation combines bioactive and bioresorbable materials, able to activate genes and to stimulate cellular responses to regenerate structures, functions and improve mechanical performance in the living tissue (HENCH, 1998, 2015; HENCH; POLAK, 2002). Biological functions and injured tissues can be enhanced or replaced with these new developments, being able to repair itself better/faster and improve quality of life from the patient (LANZA; LANGER; VACANTI, 2011).

Biomaterials are designed according to the needs, which may be a specific treatment, replacement of an organ or cosmetic use for example. The properties required for biomaterials depend on its application (RATNER et. al., 2013). They can be engineered as fibers, foams, soft and hard tissue and constructed based on metals, polymers, ceramics, living tissues and cells (NIBIB, 2017). The current use of biomaterials is linked to a range of applications such as medical implants, methods to promote healing tissues, regeneration of damage tissues, molecular probes, biosensors, drug-delivery systems, etc (HASAN et al., 2014). Nevertheless, there are issues that remain unanswered and other challenges to achieve. According to the National Institutes of Health (2017), some future directions are suggested for application of biomaterial, as: technologies to immunomodulation; injectable biomaterials to provide targeted delivery; supramolecular biomaterials that can be turned on or off in response to physiological cues or that mimic natural biological signaling.

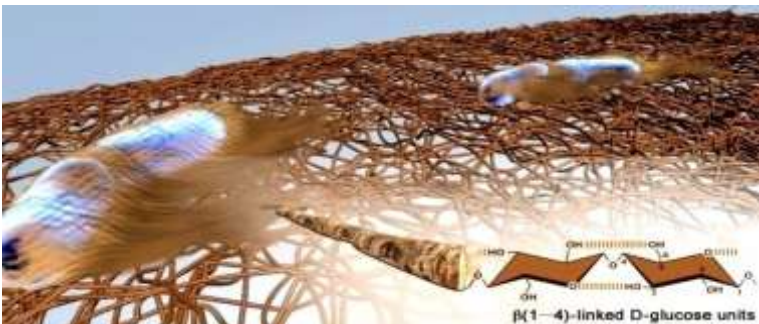
Researches in advanced composites with novel materials and structures are in a rapidly growing fashion. The positive impact these technologies might have on patients' health is immeasurable.

2.2 BACTERIAL NANOCELLULOSE HYDROGELS AS A MATRIX FOR TISSUE ENGINEERING APPLICATIONS

Cellulose is the most abundant natural biopolymer on earth, has unique properties and can be used as a starting point for transformation into new useful materials. Cellulose is present in an assortment of living species; can be synthesized by plants, some animals and a large number of microorganisms (CZAJA et al., 2004; CASTRO et al., 2011).

Bacterial nanocellulose (BNC) produced by several Gram-negative bacteria, including species of the genus *Gluconacetobacter*, is a hydrogel with 3D nanofibrils network which resembles a native extracellular matrix (ECM). BNC matrix is composed of multiple D-glucose units, interconnected by β (1 \rightarrow 4) glycosidic bonds, as showed in Figure 1 (KLEMM et al., 2005; RECOUVREUX et al., 2008; ALMEIDA et al., 2014). In terms of composition, bacterial nanocellulose is similar to plant cellulose; however, it does not present lignin and hemicelluloses in their fibers; besides, it has distinguished properties as high water holding capacity and good biocompatibility and uniformity of the nanofibers network (BARUD et al., 2011; FU; ZHANG; YANG, 2013; JOZALA et al., 2016).

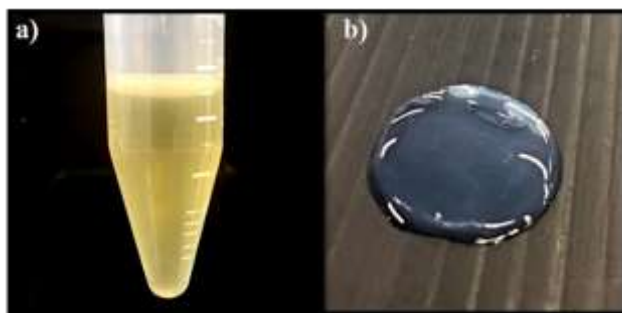
Figure 1 - Representative scheme of bacterial nanocellulose network. In detail, hydroxyl groups of nanofibers are showed



Source: BARUD et al., 2016

The nanofibers network is the result of bacterial synthesis that arises at the air-liquid interface (Figure 2-a). (KLEMM et al., 2001). When in static conditions, it forms a BNC sheet with two distinct surfaces, where the higher fiber density appears at the top surface of the culture medium (air contact); consequently, the most porous and with lower density is on the other side, the bottom surface with liquid contact (BERTI et al., 2013).

Figure 2 - Bacterial nanocellulose hydrogel (a) at air-liquid interface produced in static condition and (b) after purification.



Bacterial cellulose hydrogels can be synthesized with different shapes during *in vitro* cultures, depending on the mechanism and production method chosen (RECOUVREUX et al., 2011; NIMESKERNA et al., 2013). Colla (2014) synthesized artificial vessels from bacterial nanocellulose, where *Gluconacetobacter hansenii* bacteria grew around a silicone hose submerged in culture medium whereby oxygen was capable of diffusing through the pores of the silicone tube. Recouvreux et al. (2011) produced large three-dimensional BNC hydrogels (>150 cm³), with ellipsoid geometry via *G. hansenii* under controlled agitated culture conditions.

Studies show that BNC is used in the food, cosmetics and textile industry, in acoustics, paper production, as an emulsifier, dispersing agent, among other applications (SHI et al., 2014; WU; LIA; HO, 2013); however, biomedical use is the most promising area. Bacterial nanocellulose is applied as scaffolds in tissue engineering, due to the porous network that allows nutrient flow; are moldable and biocompatible (RAMBO et al., 2008). The potential of this polymer as a

composite is growing because of the versatility of components that can be added.

Different approaches combined bioactive particles, functional groups and antimicrobial molecules can further enhance their properties. The addition of other elements makes BNC an important matrix for new products and expands its field of application (PERTILE et al., 2012; JOZALA et al., 2016).

Table 1 - Summary of bacterial nanocellulose-based composites and their application area.

<u>Application</u>	<u>Material</u>	<u>Function</u>	<u>Reference</u>
Biomedical	Hydroxyapatite	Bone TE	Tazi et al., 2012
Biomedical	<i>Aloe vera</i>	Skin substitution	Godinho et al., 2016
Biomedical	Chitosan	Wound healing	Lin et al., 2013.
Biomedical	Keratin	Skin tissue engineering	Keskin et al., 2017
Biomedical	Bioglass	Bone regeneration	Wen et al., 2018
Electronic	Graphite	Electrical conductivity	Zhou et al., 2013
Food Industry	Nisin	Antimicrobial packaging	Nguyen et al., 2008
Food Industry	Polylysine	Biodegradable packaging	Zhu et al., 2010
Metal Industry	Chitosan	Effluent treatment	Urbina et al, 2018

BNC composites have been produced by distinct methods; *in situ*, during bacterial synthesis (SAIBUATONG; PHILSALAPHONG, 2010) or *ex situ*, modifying a pre-created BNC hydrogel (UL-ISLAM et al., 2012). Lin et al. (2013) developed a composite based on BNC and chitosan for wound dressing by *ex situ* incorporation, which allowed the adhesion and proliferation of fibroblasts. Godinho et al. (2016) synthesized BNC-Aloe scaffolds by *in situ* incorporation of *Aloe vera*, indicated as promising composite for tissue engineering and skin regeneration. Pitella (2017) modified pre-existed BNC surface by Poly-L-Lysine-Cholesterol adsorption in order to facilitate interaction with

cells; results showed an increase in the metabolic activity of human fibroblasts cultured in the new composite when compared to unmodified BNC.

Despite the increasing trend of BNC in all tissue engineering areas, the main focus continues to be in wound dressing and bone regeneration (STUMPF et al., 2018). The collagen fibers of bones are similar to those found on bacterial nanocellulose structure; this similarity and favorable mechanical stability make the hydrogel a potential material for bone tissue engineering (BTE) (HONG et al., 2006).

Recent works using BNC as a support for hard tissue engineering scaffolds have shown that the addition of HA increases the adhesion and growth of osteoprogenitor cells (ZIMMERMANN et al., 2011; TAZI et al., 2012; GRANDE et al., 2009). Honglin et al. (2016) used the BNC nanofibers structure to produce a (3D) nanofibrous bioactive glass scaffold; *ex situ* syntheses, via assisted sol-gel method, produced a calcium silicate layer on BNC nanofibers, which subsequently were calcined, remaining only a bioactive glass nanofibers.

2.3 BIOACTIVE GLASS SCAFFOLDS

In the late 1960s, many Vietnam War soldiers had limbs amputated as a result of implants rejections. Due to the need for new medical supplies, Hench et al. (1971) developed a novel material that formed a living bond with tissues in the body.

The discovery was a bioactive glass, a subset of inorganic ceramic, which is able to induce a biological response, forming strong bonds to bond through controlled surface reactions; and, has been used mostly in hard tissue reconstruction (HENCH, 1998). This glass composition contains 45wt% SiO₂; 24.5wt% Na₂O; 24.5wt% CaO and 6wt% P₂O₅, designated as 45S5 bioactive glass (BG), and commercial named Bioglass®.

Since this initial development, the investigation of bioactive ceramics has increased. New materials and products from variations on bioactive glasses, synthetic hydroxyapatite (HA) and other calcium phosphates have been characterized (HENCH, 2009; LEGEROS, 2002).

The arrangements based on SiO₂-Na₂O-CaO-P₂O₅, are similar to the natural bone components, have the ability to form a bone-like hydroxyapatite layer on its surface, enhance osteoblasts cell growth as an osteoprogenitor material, and are well-known as bone regenerative scaffolds (MCMANUS et al. 2005; HUANG et al. 2007; XU et al.,

2011). The growth of HA layer along the implant interface is closely associated with osteoconduction; the higher the growth rate, the faster the material will attach to the bone (JONES et al., 2013).

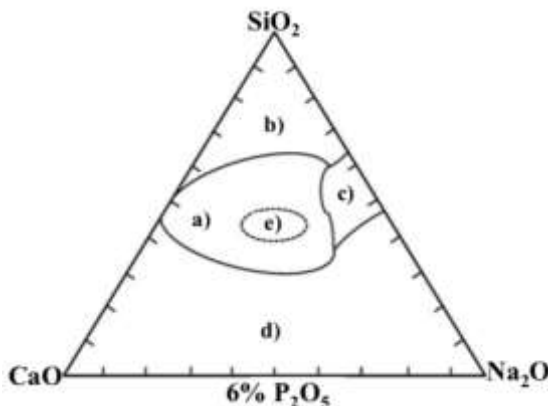
A classification has been proposed by Hench (2006) to differentiate the bioactivity of materials. Two classes were set according to its behavior:

Class A - enhance new bone formation (osteoinductive) and have osteoconductive abilities, activating intra and extra cellular response;

Class B - only promote an extra cellular response, defined as osteoconductive.

Figure 3 shows the compositional dependence of bone bonding to bioactive glasses, where just small part has double response as osteoconductive and osteoinductive behavior. Furthermore, there are arrangements that will not form a glass and others that will not bond to the tissue (HENCH, 2015). Bioglass® lies in the center of the compositional diagram, as Class A biomaterial.

Figure 3 - - Compositional dependence of bone bonding regions for bioactive glasses. The regions represent: (a) Class B glasses; (b) and (c) non-bonding glasses, where reactivity are too low and too high, respectively; (d) non glass forming; and (e) Class A glasses.

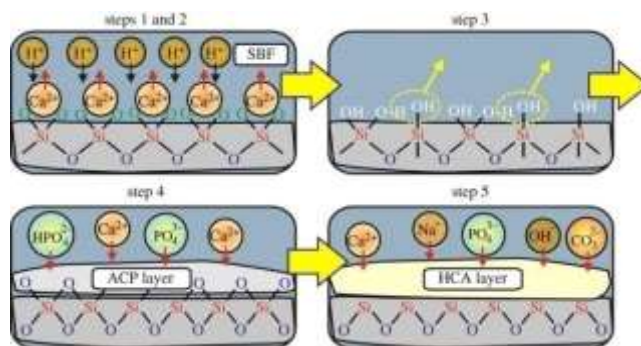


Source: Adapted from HENCH, 2015.

Bioactivity of bioactive glasses has been shown to be directly connected to the formation of a HA layer, interacting with collagen

fibrils of the bone to form a bond (HENCH, 2006). *In vitro* studies of this mechanism use a simulated body fluid (SBF) to mimics the blood plasma, a protein-free and acellular solution developed by Kokubo (1990). This mechanism involves the rapid release of soluble ionic species from the bioactive glass and form a hydroxyl carbonate apatite (HCA) layer on its surface, as proposed at the schematic illustration (Figure 4) and at Table 2.

Figure 4 – Schematic illustration of HCA formation from a bioactive glass exposed to SBF.



Source: Gunawidjaja et al., 2012

Table 2 – Mechanism stages in HA formation on the bioactive glass surface.

STEP	PROPOSED STAGES FOR HA FORMATION
1 and 2	Ca ²⁺ ↔ H ⁺ exchange, creating bonds (Si–OH) on the glass surface
3	Repolymerization of silica layer: 2Si–OH → Si–O–Si + H ₂ O
4	Formation of amorphous calcium phosphate (ACP) on the silica gel
5	ACP → HCA crystallization

In order to measure an *in vivo* bioactivity, Hench (1991) also proposed an index, $IB=100/t_{50bb}$, related to the time for more than 50% of the material interface to be bonded (t_{50bb}). Bioglass[®] is the most

bioactive material, with an index of bioactivity $IB=12.5$, comparing to the HA that presents $IB=3$ and inert ceramics with $IB=0$. Studies also revealed that Bioglass[®] allowed the complete recovery of bone after only two weeks, comparing to HA that took twelve weeks to produce a correlate response (OONISHI et al., 1999), which makes BG more suitable for bone tissue engineering (BTE).

The subsequent steps of glass bonding reactions are influenced by Si and Ca ions, stimulating genes expression of osteogenic precursor cells and influencing their proliferation cycle (VARGAS et al., 2009). This process, named osteoinduction, favors osteoblasts differentiation and produces ECM proteins, as collagen type I and osteocalcin (XYNOS et al., 2000, 2001) that mineralizes as a regenerated bone (BERGERON et al., 2007). New approaches for enhancing bioactivity of scaffolds are being investigated by introducing drugs and stimulant ions (DU; XIANG, 2012). Furthermore, bioactive glasses have been shown to increase the secretion of VEGF and FGF *in vitro* (DAY, 2005; GORUSTOVICH; ROETHER; BOCCACCINI, 2010), and enhanced the growth of blood vessels from pre-existing ones (angiogenesis) and new ones (vascularization) (HENCH; POLAK, 2002). These features are beneficial for wound healing applications and offer the potential for soft tissue regeneration (HENCH et al., 1971; HENCH, 2009; HOPPE; GULDAL; BOCCACCINI, 2011).

Currently, there is a wide range of bioactive glasses used in biomedical products. Bioglass[®] was approved by Food and Drug Administration (FDA) in 1985, and since then more than 1.5 millions of patients received this material to repair their bone and dental defects (JONES et al., 2016). The first implant for clinical use was for the replacement of middle ear small bones (MEP[®]) based on 45S5 bioactive glass; other device was the Endosseous Ridge Maintenance Implant (ERMI[®]), still applied today in periodontal surgery. Other examples of commercially products are TheraSphere[®], insoluble glass microspheres for cancer treatment (BASKAR et al., 2012); DermaFuse[™]/Mirragen[™] for healing of long-term venous stasis ulcers (JUNG et al., 2011); NovaMin and PerioGlas[®] for treating dental hypersensitivity and periodontal disease, respectively (PRADEEP; SHARMA, 2010).

Despite of various excellent properties, the major disadvantage of bioactive glasses porous scaffolds is their poor mechanical properties in load bearing applications (GERHARDT; BOCCACCINI, 2010; CHEN et al., 2014). This drawback becomes even more critical in a highly porous scaffold or when the degradation begins, restricting the use of

BG scaffolds in some applications (CHEN et al., 2006, 2014). As a result, studies to produce bioactive glass with optimized attributes are reported, combining molecular modifications and a variety of bioactive composites based in metals or polymers (YUNOS et al., 2008; EQTESADI et al., 2016; HENRIQUE et al., 2017).

2.4 COMPOSITES FOR BIOLOGICAL APPLICATIONS

In order to improve materials properties and well performance, development of composites are made by combining two or more types of materials, minimizing their short comings and providing better physical, biological or mechanical attributes for specific applications (CHEN et al., 2006).

Composite systems linking polymers and ceramics can provide reinforced characteristics to fabricate scaffolds for soft and hard tissue engineering (RAMBO et al., 2006; YANG et al., 2012). Peter et al. (2010) prepared a nanocomposite scaffold of chitosan-gelatin- bioactive glass, which indicated better properties and provided a healthier environment for cell proliferation. Ran et al. (2017) designed multi-component composite for bone tissue engineering based on bacterial nanocellulose-gelatin-hydroxyapatite; the results showed higher proliferation and differentiation potential for mesenchymal stem cells when compared to BNC-gelatin and BNC-HA.

2.5 TISSUE ENGINEERING

Tissue engineering involves interdisciplinary fields, applying principles of life sciences, cell culture, engineering and material science, with set of methods to develop substitutes that will enhance biological functions or replace damaged tissues (RAMBO et al., 2006; LANZA; LANGER; VACANTI, 2011).

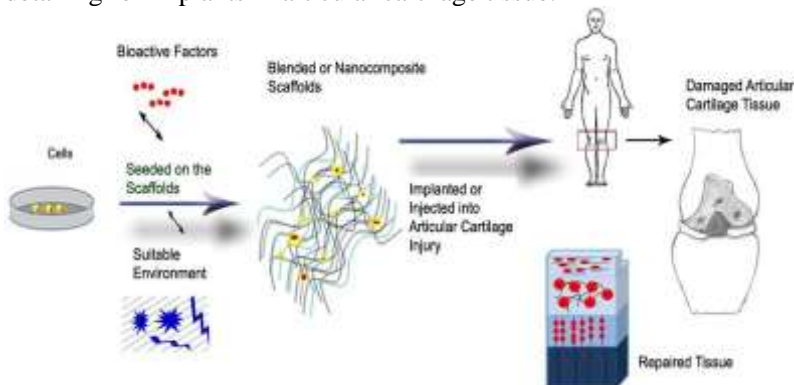
The applications of TE include healing systems, where specialized supports, assembled or not with cells, are implanted to promote local tissue repair (GRIFFITH; NAUGHTON, 2002); further to clinical functions, other uses include diagnostic screening, as models to study efficacy and toxicology of drugs (BERTHIAUME; MAGUIRE; YARMUSH, 2011). The progresses in this area will allow prevention, diagnosis and molecular treatment of diseases (HORCH et al., 2012).

Tissues consist of cells, the ECM and signaling systems; the premise of TE is to mimic a specific tissue, hence any engineered scaffold should have a similar triad of components (CHAN; LEONG,

2008). Systems of production of tissue engineering scaffolds utilize different approaches. The process can use living cells from the own patient, from another donor (allogenic source), or donors from different species (xenogeneic), to grow on a three-dimensional scaffold and then be implanted (GRIFFITH; NAUGHTON, 2002). The second approach involves acellular scaffold combined with growth factors; when implanted, it will recruit the cells from de patient to form the tissue (RICHARDSON et al., 2001). These concepts can also be aggregated by addition of cells and growth factors as shown in Figure 5.

In order to provide an ideal environment, to mimic the extracellular matrix, scaffolds containing ceramics, polymers and metals have been designed to favor the formation or regeneration of different tissues. Furthermore, ideal scaffolds must afford the microenvironment to cellular interaction, proliferation and differentiation, allow diffusion of nutrients, and also support mechanical loads, similar to the native tissue (SERPOOSHAN et al., 2010; DOULABI; MEQUANINT; MOHAMMADI, 2014). Generally developed to be gradually biodegraded and eventually disintegrate and dissolve until it reaches the purpose (REZWAN et al., 2006).

Figure 5 –Schematic representation of the tissue engineering procedure, detailing for implants in articular cartilage tissue.



Source: Doulabi; Mequanint; Mohammadi, 2014

Engineering challenges are limiting scaffolds functionality; once implanted, the major challenge is blood nutrients supply, because cells consume the available oxygen in hours and take several days to form new blood vessels (KAULLY et al., 2009; LOVETT et al., 2009). To overcome this limitation, incorporation of functional groups, active

proteins, drugs, growth factors are important to success; likewise, porous structures are crucial, allowing mass flux and larger surface area for cell proliferation (CHEN et al. (2006).

The main applications and targets are those tissues that are prone to disease, degeneration and traumas; including skin, vascular system and bone tissues. Therefore, the results of TE field may improve the lives of millions of patients and have a huge economic impact.

2.5.1 Bone tissue engineering

The approach to bone tissue engineering aims to restore function of diseased or damaged bone tissue. Bone is a complex tissue with several cell phenotypes, distinct porosities, high vascularization and requires a high mechanical role (DENG; LIU, 2005; BACKER et al., 2009). The mineral matter of bone is hydroxyapatite and the organic part consists mainly of collagen fibers and also noncollageneous proteins (SHOICHET et al., 2010).

A potential bone tissue engineering (BTE) scaffold depends on several factors, should present biocompatibility, osteoconductivity, osteoinductivity, bioactivity, to be mechanically compatible with native soft or hard tissue and present a porous structure in order to integrate with the native structure. The manufacturing of these scaffolds should cover several shapes to match with specific defects and also be suitable for commercialization (JOHNSON; HERSCLER, 2011). Assorted materials have been examined in this area and include ceramics, metals, polymers and composites arrangements. Recently, nanomaterials have emerged as promising components owing to their potential to mimic the natural ECM and replace damaged bone tissues (ZHAO et al., 2013).

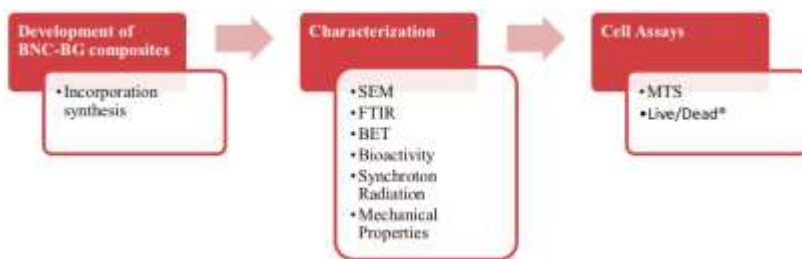
There are several reasons to focus the attention to bone regeneration approaches; bone defects caused by trauma, infection or cancer are difficult to repair surgically and affect an enormous number of patients.

Based on these references, it is proposed the development of a novel composite based on BNC-BG, integrating the properties of those materials as a scaffold for soft and hard tissue engineering.

3 MATERIALS AND METHODS

This chapter is composed of three parts, which describe the materials and methods of this study. The first section introduces the synthesis of the BNC-BG composites; second and third describe the characterization analyses of the scaffold and *in vitro* cell assays, respectively. The diagram of the main stages performed is shown in Figure 6.

Figure 6 - Diagram representing the structure of this work and the experiments performed.



3.1 DEVELOPMENT OF BNC-BG POLYMERIC COMPOSITES

3.1.1 BNC hydrogel synthesis

Bacterial nanocellulose hydrogels were synthesized by *Komagataeibacter hansenii* (ATCC 23769). The bacteria were cultured in Mannitol medium, composed of 25.0 g·L⁻¹ mannitol, 5.0 g·L⁻¹ yeast extract and 3.0 g·L⁻¹ bactopectone, pH 6,5 and sterilized by autoclaving (121 °C for 20 min).

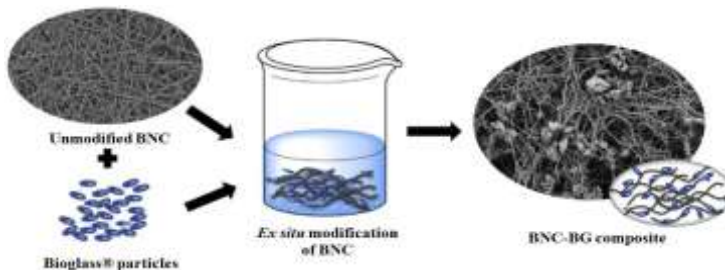
K. hansenii inoculum was spread onto mannitol agar plates and incubated at 26 °C for seven days to form isolated colonies. Bacteria colonies were suspended in 10% v/v of Mannitol medium until an optical density equals to 1 (OD=1) at 660 nm was obtained; subsequently the remainder medium was included and then transferred to 24 wells plates (2 mL/well) for the biosynthesis. During the hydrogels production, cultures were maintained at 26 °C under static growing conditions. After 7 days, BNC membranes were removed and purified in 0.1 M NaOH solution at 50°C for 24 h and later rinsed with distilled water to pH 6.5. Finally, the hydrogels were sterilized by autoclaving (121 °C for 20 min) and kept refrigerated until use.

3.1.2 *Ex situ* incorporation of Bioglass® into BNC hydrogels

The bioactive glass utilized in this work was a melt-derived 45S5 Bioglass® powder (particle size 2 to 5µm) by SCHOTT Vitryxx®, Germany.

In order to enhance BNC properties, BG particles were integrated by *ex situ* modification method (Figure 7) into the polymeric matrix. Pre-synthesized BNC scaffolds were soaked into three solutions based on different proportions of distilled water and ethanol p.a., which contained BG particles (1 % w/v). After predetermined times, under magnetic stirring (360 rpm) and room temperature, BNC-BG composites were removed and sterilized in water by autoclaving (121°C for 20 min).

Figure 7 – *Ex situ* incorporation of BG particles onto the unmodified BNC hydrogels.



Source: Adapted from STUMPF et al., 2018

The bacterial nanocellulose-Bioglass® composites synthesized were identified according to their coating solution, as shown in Table 3.

Table 3 – Identification of the composites according to the coating solution.

TYPE	SOLUTION	COMPOSITE
1	Water	BNC-BG
2	25%EtOH	BNC-BG – 25%EtOH
3	50%EtOH	BNC-BG – 50%EtOH

3.2 CHARACTERIZATION OF BNC-BG COMPOSITES

3.2.1 *In vitro* bioactivity of BNC-BG composites

According to the standard technique, *in vitro* bioactivity of BNC-BG composites was investigated by immersing the scaffolds in simulated body fluid and examining the deposition of hydroxyapatite on their surface.

SBF solution was prepared according to Kokubo (Kokubo 1990, 2006). A range of reagents was dissolved one at a time in 1L of deionized water. First amount of chemical is 7.9948g of NaCl, followed by 0.3543g of NaHCO₃, 0.2250g KCl, 0.2310g K₂PO₄·3H₂O, 0.3042g MgCl₂·6H₂O, 39 mL HCl (1M), 0.3623g CaCl₂·2H₂O, 0.0720g Na₂SO₄ and 6.0508 mL of Tris; then, the SBF solution is buffered at pH 7.4 using HCl.

The composites were placed in tubes, immersed in 50 mL of SBF and maintained at 37 °C in a shaking incubator (90 rpm). After each time point, the composites were rinsed with deionized water and dried at supercritical carbon dioxide (scCO₂) for further analysis.

3.2.2 Scanning Electron Microscopy (SEM) with Energy Dispersive Spectroscopy (EDS)

The surface morphological analyses of the composites were assessed by scanning electron microscopy (SEM (Auriga –Carl Zeiss, Germany)). Samples were dried with scCO₂ dryer and gold-sputtered before observation at an accelerating voltage of 1.20 kV. Samples composition, after SBF contact, were analyzed by EDS associated with SEM, where X-ray energy spectrum at a position provides plots of the relative elemental concentration.

3.2.3 Chemical characterization of BNC-BG composites

Fourier transform infrared spectroscopy (FTIR; Nicolet 6700, Thermo Scientific) was used to analyze the chemical structure of BNC-BG. The spectra were recorded in a range of 4000–500 cm⁻¹, using attenuated total reflectance. This test was carried out on samples before and after immersion in SBF.

3.2.4 Characterization of the surface area and pore volume of BNC and BNC–BG hydrogels

Brunauer-Emmett-Teller (BET) analysis (Quantachrome Autosorb 1) provides a specific surface area assessment of BNC and BNC-BG scaffolds by nitrogen adsorption/desorption at 77 K. Pore size distribution of pores were performed by the Barrett– Joyner–Halenda (BJH) equation.

3.2.5 Mechanical properties measurement

The mechanical parameters, including tensile strength, elongation at break, and Young's modulus of BNC and BNC-BG were determined on a Stable Micro Systems Texture Analyser (Model–TA–HDplus) using a 500 N load cell at room temperature. Wet BNC and BNC-BG hydrogels with dimension of 90x15x0.5 and 90x15x0.09 mm, respectively, were mounted between the grips of the machine. The initial grip separation (Figure 8) was 30 mm and cross-head speed was set to 1 mm/s.

Figure 8 - Samples fixation for tensile strength test.

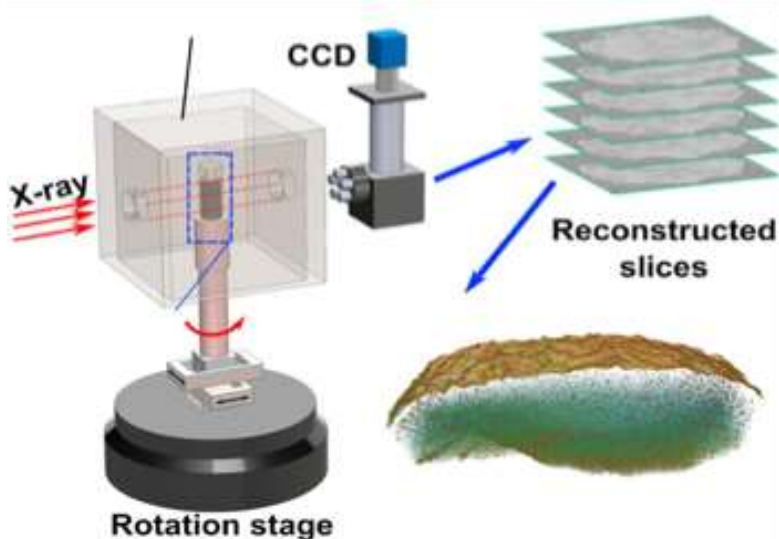


3.2.6 Synchrotron Radiation

Synchrotron computed tomography was performed at the Diamond Manchester Branchline (I13-2) by Diamond Light Source. Polychromatic X-rays with energy in the range of 8–35 kV filtered with

C and Al filters. Over 3600 projections were recorded over 0 to 180° rotation and exposure of 0.05 ms using a scintillator coupled PCO edge camera with $2,560 \times 2,160$ detector array, giving an effective pixel size of $0.33 \mu\text{m}$. Filtered back projection was applied to reconstruct the projections using codes developed at Diamond Light Source (Atwood et al., 2015), as showed the scheme at Figure 9. The resulting tomographies each comprise $2,560 \times 2,560 \times 2,160$ voxels with an effective voxel size of $0.33 \mu\text{m}$ were processed using ImageJ and a commercially available software Avizo®. These analyses were gently carried out by Dr. Felipe Perozzo Daltoé, in collaboration with Dr. Gowsihan Poologasundarampillai from the University of Manchester, UK.

Figure 9 – Schematic experimental set-up on the Diamond-Manchester Branchline and typical results.



Source: Adapted from SHUAI et al., 2016

3.3 IN VITRO ASSAY

To evaluate the biocompatibility of BNC hydrogels incorporated with BG particles, *in vitro* tests were performed using fibroblasts and preosteoblasts cell lines.

3.3.1 Cell culture

Immortalized murine fibroblast cells (L929), and mouse preosteoblast cells (MC3T3-E1), were cultured in treated plates using Dulbecco's Modified Eagle's Medium (DMEM) (Gibco®) and alpha minimum essential media (αMEM) (Gibco®), respectively; culture medium was supplemented with 10% (v/v) fetal bovine serum (FBS) and 1% (v/v) antibiotics penicillin/streptomycin. Cells were incubated at 37 °C, in a humidified atmosphere with 5% CO₂. After about 80% confluence, cells were detached using trypsin solution and centrifuged, then resuspended in complete medium for further seeding and experimental analysis.

3.3.2 Viability and proliferation of fibroblast cells

Sterile BNC hydrogels and BNC-BG composites were placed in culture plates and kept in DMEM medium for 24 h in humidified atmosphere (5% CO₂); then, the medium was removed and L929 fibroblasts were seeded onto the materials at a density of approximately 105 cells/well. The medium was not replaced during the culture time. Progressive cell proliferation was analyzed after 1, 3 and 7 days by a colorimetric mitochondrial activity assay (Cell Titer 96® Aqueous One Solution Proliferation Assay, Promega, USA), based on 3-(4,5-dimethyl-2-yl)-5-(3-carboxymethoxyphenyl)-2-(4-sulphophenyl)-2H-tetrazolium (MTS).

In the MTS assay, samples were washed three times with PBS and transferred to a new plate, soaked with 300 μL of culture medium and 60 μL MTS reagent. Culture plates were incubated, protected from light, for 2 h at 37 °C in 5% CO₂ atmosphere. Past the set time, the solution was homogenized, and transferred (in triplicate) to a new 96-well culture plate; then, absorbance (OD value) of supernatants solutions was measured at 490 nm (Micro ELISA reader). Cytotoxic potential of BNC-BG hydrogels was evaluated following the direct contact assay, according to the International Standardization Organization 10993-5 (ISO, 2009), based on unmodified BNC hydrogels as control.

Viability of the L929 cells cultured on BNC and BNC-BG hydrogels after 7 days was also determined by Live/Dead® assay (Life Technologies Corporation, Carlsbad, CA, USA). Living cells are distinguished from dead cells by calcein, which produces a uniform fluorescent green color; the ethidium homodimer (EthD) enters the cells

with damaged plasma membrane, interacts with the DNA and presents a fluorescent red color to dead cells. The hydrogel samples were washed several times with PBS, transferred to a new plate and a solution combined Live/Dead® reagents (4 μ M of EthD and 1 μ M of calcein in PBS) was added, 500 μ L per well. After 30 minutes at room temperature, samples were analyzed under a fluorescence microscope (Nikon Eclipse Ci-L, Japan).

A second proliferation procedure was prepared, similar to the one described above, where L929 cells were seeded directly on the 24-well culture plate with a density of 2×10^4 cells/well for 24 h in an incubator at 37 °C with 5% CO₂ atmosphere. After 24h, BNC hydrogels, BNC-BG (15 mg BG per membrane) and BNC-BG5min (2 mg BG) composites were added into each well. After 1, 3 and 7 days *in vitro*, MTS assay was performed as previously; however, the membranes were discarded and the procedure was done in the same culture plate. In this case, the aim was to analyze cell viability and proliferation in different concentrations of BG in the composite. BNC were used as positive control and cells as the negative control.

3.3.3 Metabolic activity of MC3T3-E1

A MTS Cell Viability Assay Kit was used to quantify the metabolic activities of preosteoblasts with an absorbance reader; the procedure is similar to the one previously described.

Sterile BNC hydrogels and BNC-BG composites were placed in culture plates and kept in α MEM medium for 24 h in humidified atmosphere (5% CO₂); then, the medium was removed and MC3T3-E1 preosteoblasts were seeded onto the materials at a density of approximately 105cells/well. For analysis, proliferation was analyzed after 1, 3 and 7 days *in vitro* culture by MTS assay as described.

3.3.4 Statistical analysis

Data were statistically analyzed by one-way analysis of variance (ANOVA) with Tukey test. Values represent the mean \pm standard medium error, with $p < 0.05$.

4 RESULTS AND DISCUSSION

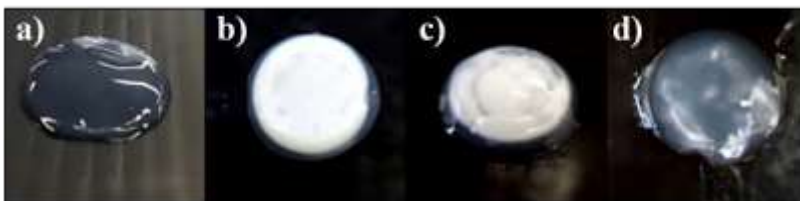
4.1 PRODUCTION BNC-BG COMPOSITES

In order to synthesize a new composite, three tested solutions were compared based on the amount of BG particles incorporated into the membranes, considering the same time interval.

BNC hydrogels were soaked during one day in different solutions to incorporate Bioglass®, then BNC-BG, BNC-BG-25%EtOH and BNC-BG-50%EtOH composites were produced; the amount of BG particles inside the membrane was much higher and homogeneous when BNC matrices were synthesized in a solution without ethanol, as shown in Figure 10.

Differences were observed macroscopically, revealing that the higher concentration of ethanol, the less BG incorporation into the hydrogel. This is due to organic solvents significantly reducing the solubility of the glass (KACPERSKA, 1994; ROMEIS et al., 2015). Such variation is suggestive of the chemical bonds between the components, attributing better connection to BNC-Bioglass® in water, as detailed in Figure 11.

Figure 10 – Photographs of a) BNC hydrogel before incorporation and BNC-Bioglass® after 1 day soaked in b) water, c) 25%EtOH and d) 50%EtOH solutions with BG particles (1% w/v).



Similar scaffolds already have been synthesized, usually with HA as inorganic component (GRANDE et al., 2009; SASKA et al., 2011; ZIMMERMANN et al., 2011); however, a hydrogel composite based on BNC- Bioglass® is a novel material.

Figure 11 - Photography showing the detailed BNC-BG composite; synthesized after 1 day in water soaking solution with 1% w/v of BG particles.

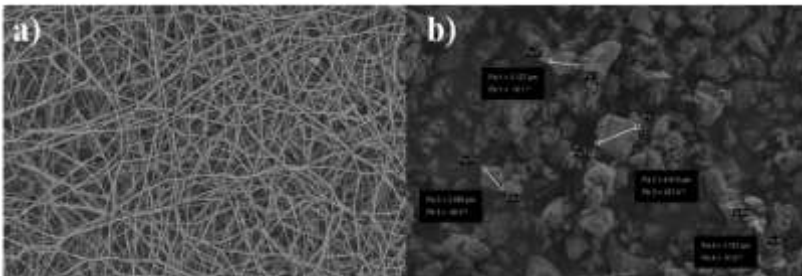


4.2 CHARACTERIZATION OF BNC-BG COMPOSITES

4.2.1 Morphological behavior

The distribution of BG in the BNC matrix was analyzed by scanning electron microscopy (SEM). Both materials were characterized separately before the synthesis of the composites, and shown in Figure 12.

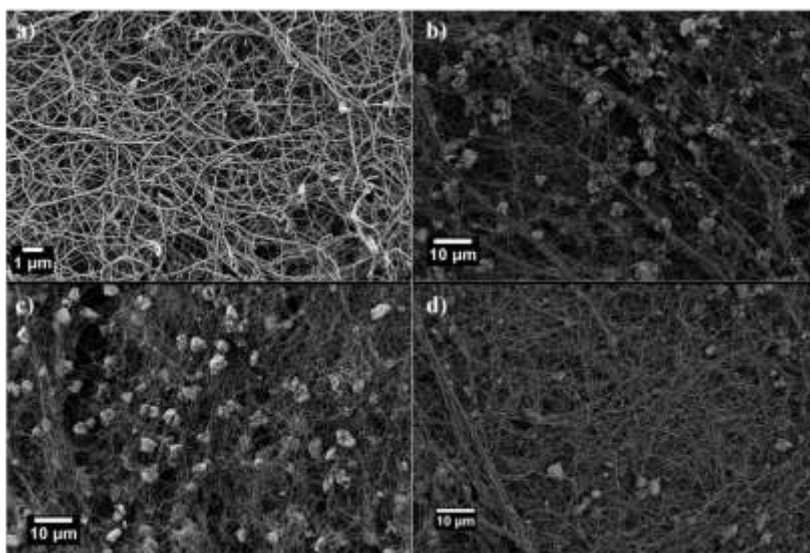
Figure 12 – SEM images from (a) pure BNC membrane, and (b) BG particles and their random sizes.



SEM images, even with high magnification, confirm macroscopic differences; where smaller amount of BG particles have been incorporated into BNC matrix with 50% v/v alcohol in the synthesis solution (Figure 13). BNC-BG (Figure 13-b) and BNC-BG-25%EtOH

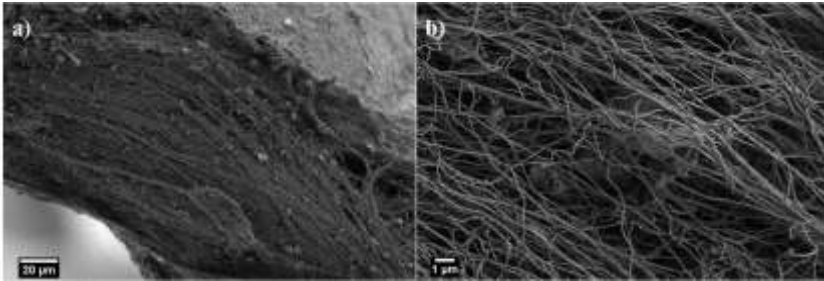
(Figure 13- c), not much difference was observed even when analyzed punctually using a magnification of 2000x, and demonstrated a homogeneous distribution of BG particles covering the BNC porous surface.

Figure 13 –SEM micrographs of (a) unmodified BNC fibers; (b), (c) and (d) BNC-bioactive glass composites after 24 hours soaked in water with 0; 25 and 50% v/v of ethanol, respectively. Homogeneous distribution of BG particles covers the BNC surface in BNC-BG (b) and BNC-BG-25%EtOH (c).



In Figure 14, the cross-section images of the composite confirmed the presence of BG particle ingrained between the nanofibers. This fact might have occurred due to the stirring forces during the synthesis, and the particles disrupted some of the BNC nanofibers.

Figure 14 - (a) Cross section of the BNC-BG composite. In detail (b), BG particle ingrained between the nanofibers.



4.2.2 Fourier transforms infrared spectroscopy

FTIR analyses were performed to characterize the molecular composition of the materials and to evaluate the influence of the solvent system on the structure of the BNC-BG composites. Results are shown in Figure 15.

The spectra of BNC is observed by characteristic peaks, where the region $3200\text{--}3500\text{ cm}^{-1}$ is related to hydroxyl groups of cellulose (FENG, et al, 2012; KUMAR et al, 2017); the second band, at 1427 cm^{-1} is characteristic of HCH and OCH; band at 1379 cm^{-1} is related to CH bending and 1161 cm^{-1} band is characteristic of asymmetric C-O-C stretching; the peak at 1109 cm^{-1} is a symmetric vibration of C-C; 1040 and 1063 cm^{-1} are from C-O stretching band (ASHORI et al., 2012; ZHONG; QIN; MA, 2015). The vibrational band at 670 cm^{-1} is related to COH (STUMPF et al., 2013).

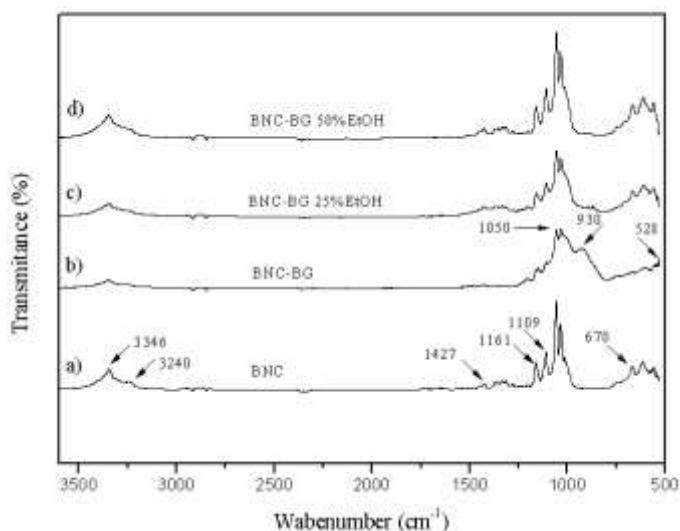
For BNC-BG composites (spectra b–d), it is more evident the changes when in water solution (Figure 15-b), where it is possible to see from $530\text{--}670\text{ cm}^{-1}$ the characteristics of phosphate group ($\text{PO}_4\text{--}3$), at 930 cm^{-1} vibrational band is characteristic of stretching Si-OH and at the double peaks around 1050 cm^{-1} is attributed to phosphate group ($\text{PO}_4\text{--}2$) with SiO_2 stretching band. These bands in the spectrum are from Bioglass®. In addition, the O-H and C-O-C/C-O bands of the cellulose reduced intensities are around $3200\text{--}3500\text{ cm}^{-1}$ and $1160\text{--}1050\text{ cm}^{-1}$, respectively. This result is in good agreement with similar works previously reported (ASHORI et al, 2012; BARUD, 2008; SASKA et al, 2011).

It is clear that using different solutions with the same quantity of BG particles it affects the incorporation to the composite. Furthermore,

based on the width and intensity changes of the phosphate absorption bands, it is indicated that as ethanol content increases, less BG particles are adsorbed and encapsulated by BNC membranes.

The advantage of the synthesis solution containing only water is to incorporate BG with better efficiency: 15 mg of BG particles were immobilized in BNC by water solution, approximately 93% of BNC dry weight.

Figure 15 – FTIR results of (a) unmodified BNC (control) and BNC+BG composites soaked in (b) water; (c) 25% v/v EtOH solution and (d) 50% v/v EtOH solution.



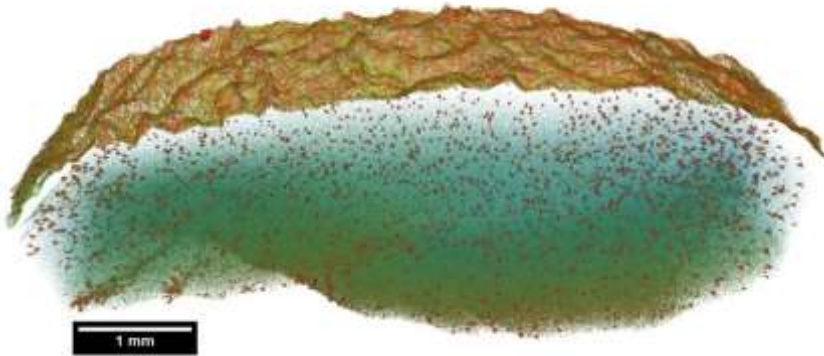
Based on results from *ex situ* incorporation syntheses images and FTIR spectra, BNC-BG composites coated in water were used for the subsequent detailed characterization and *in vitro* studies.

4.2.3 Synchrotron X-ray tomography

Synchrotron X-ray tomographic microscopy was used to elucidate the 3D structure of BNC-BG composite. Figure 16 shows cross-section of BNC-BG synthesized in water, demonstrating a uniform distribution of the particles throughout the entire hydrogel volume. The determination of the diameter was performed by its local thickness,

where reddish colors in the scaffolds indicate thicker than the blue/green ones (SHUAI et al., 2016).

Figure 16 – 3D volume rendering of the BNC-BG hydrogel, composed of cross-sectional stacked images. Homogeneous dispersion of the particles inside the membrane is observed.



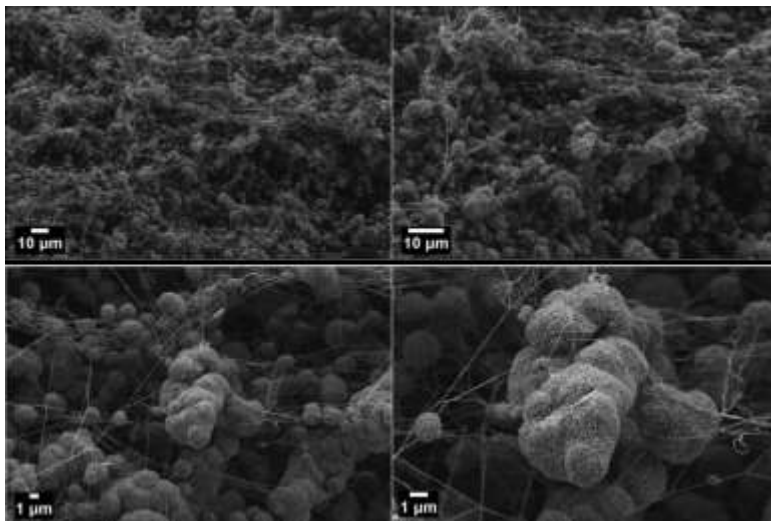
4.2.4 *In vitro* bioactivity of BNC-BG composites

The ability to form a carbonated apatite layer when in simulated body fluid is an indicative of bioactivity (KOKUBO et al., 1990). To evaluate the bioactivity of the sintered BNC-BG composites, the surface of the materials was examined by SEM and FTIR after *in vitro* SBF immersion.

After 1 day of SBF exposure, all the tested samples exhibited signs of surface dissolution, increasing their surface roughness due to apatite formation, revealing that BNC-BG composites had a HA formation ability. Figure 17 shows the SEM micrographs of the BNC-BG after it was immersed in SBF. Several magnification increments were used to analyze BG surface. Figure 17 (a-d) showed magnification of 1,000x, 2,000x, 5,000x and 10,000; respectively.

The EDS spectrum shown in Figure 18 confirmed that the layer formed on these glasses is rich in Ca and P, corresponding to the compositions of hydroxyapatite $\text{Ca}_{10}(\text{PO}_4)_6(\text{OH})_2$.

Figure 17 SEM images of BNC-BG after 1 day in simulated body fluid. Micrographs (a), (b),(c), and (d) showed magnification of 1,000x, 2,000x, 5,000x and 10,000, respectively.



The morphologies of the composites after 7 days in SBF are shown in Figure 19. It is recognized that the hydroxyapatite structure layers formed on BG the surfaces inside the composite are denser and more visible after 7 days in SBF. This confirms the effective crystallization of apatite layer on BG surface.

Figure 18 – Results of EDX analysis for BNC-BG composites after 7 days in SBF showing elemental surface mapping of the HA layer.

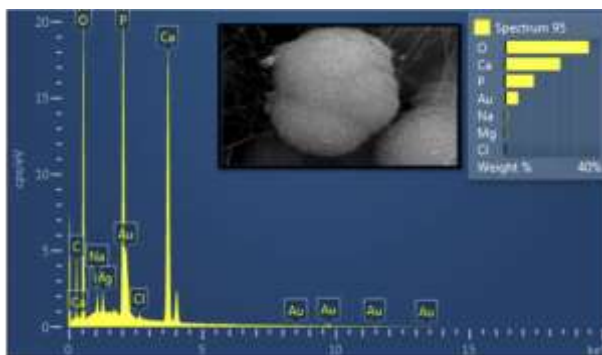


Figure 19 - SEM images of BG particles after (a), (b) 1day in SBF, magnification of 30,000x and 80,000x, respectively; and (c), (d) 7 days in SBF using magnification of 30,000x and 80,000x, respectively. A denser HA layer can be seen after a longer time.

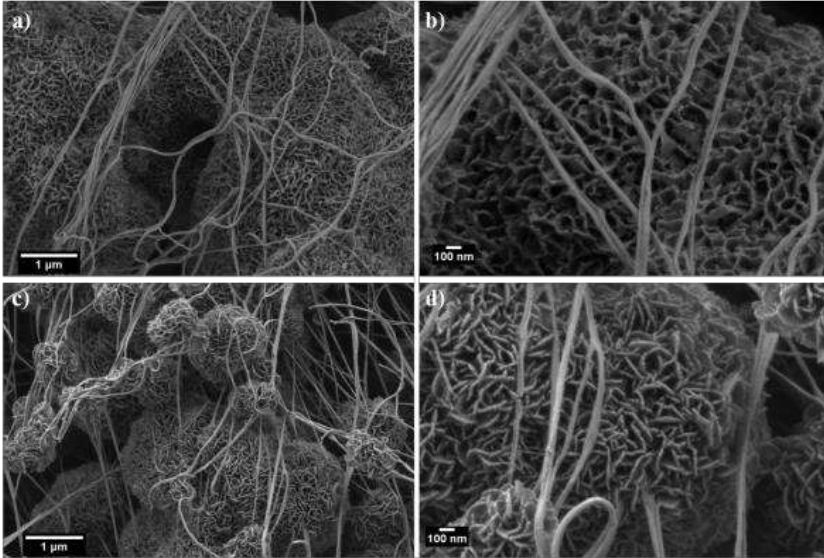
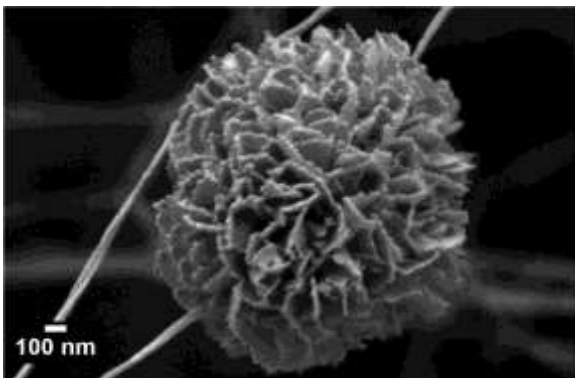


Figure 20 shows an SEM image with an increase of 80,000x, where HA crystal is formed between a single cellulose nanofiber.

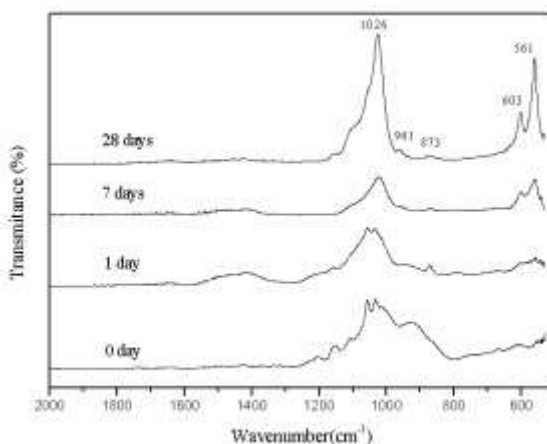
Figure 20 SEM micrograph of a detailed HA crystal on the nanofibers of BNC (80,000 × magnification).



FTIR spectra of the BNC-BG membranes before and after immersion in SBF are presented in Figure 21. After soaking in SBF solution, the characteristic bands are strongly modified due to reactions between BG and the simulated body fluid (OUDADESSE et al., 2011). The changes as days go by are perceptible; after 28 days the composite reveals new peaks at 961 and 1026 cm^{-1} corresponding to phosphate bands (P-O stretch); and two peaks at 561 and 603 cm^{-1}

to the P-O bending vibrations of hydroxyapatite (EROL et al., 2012). A C-O stretching vibration band also appeared at 873 cm^{-1} , suggesting the formed HA was carbonated hydroxyapatite (ZHU, KASKEL, 2009; LIU, RAHAMAN, DAY, 2013). The peaks attributed to silica gradually decreased and disappeared and this result confirms the crystallization of the apatite on the glass surface of the composite, which is the marker for bioactivity in the context of materials for bone tissue engineering (HENCH, 2009; LIEN; KO; HUANG, 2010).

Figure 21 – FTIR spectra of BNC-BG synthesized in water solution, before and after immersion in SBF.



4.2.5 Characterization of the surface area and pore volume of BNC and BNC-BG hydrogels

Nitrogen adsorption-desorption experiments were performed to examine the surface area and pore volume of the scaffolds; data of both samples are given in Table 4. In addition,

SEM images (Figure 22) present porous structures and distribution of BG particles in the composites.

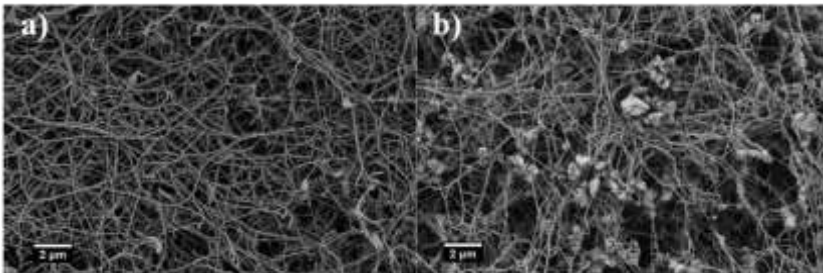
Table 4 - Surface area (SA) and pore volume (PV) of BNC and BNC-BG hydrogels.

Sample	SA (m ² /g)	PV (cm ³ /g)
BNC	417.1	0.52
BNC-BG	598.1	0.91

The specific surface area of the materials increased approximately 43% after the adsorption of bioactive glass particles into the membrane. This result is due to rough covering of the BNC nanofibers, forming a higher SA on the 3D sample (SAIBUATONG; PHISALAPHONG, 2010; UL-ISLAM; KHAN; PARK, 2012). Pore volume for the BNC-BG

composite is quite different from the unmodified membrane, which value is 74% higher comparing to BNC. Figure 22 confirms pore volume modification, where larger pores are detected after the incorporation. It indicates that particles penetrate through the BNC pores and possibly expand these pores deep in the interior; this fact might occur due to the stirring forces during synthesis procedure.

Figure 22 – SEM images showing surface morphologies and pores, for: control BNC; and BNC-BG composites.



Similar to these results, a composite based on BNC with inorganic clay particles (montmorillonite) have higher surface area than that of the pure BNC matrix, showing 370 m²/g and 285 m²/g, respectively; that could be due to irregular arrangement of clay particles on the surfaces of BNC hydrogel (UL-ISLAM, KHAN, PARK, 2012). Moreover, another BNC based composite was modified by addition of alginate and showed an increase of the surface area by about 84%, from 19.97 to 36.76 m²/g. The total pore volume also increased from 0.077 to 0.23 cm³/g from BC to BNC-Alginate, a change of 200% (CACICEDO et al., 2018). Similarly, a nanoscale network structure composed of silica gel and bacterial cellulose was designed; the composites with a high content of SiO₂ (approx. 80-90%) showed surface area of nearly 800 m²/g, compared to 108 m²/g from the unmodified matrix (SAI et al., 2018).

It has been shown that the *ex situ* modification process used for BG incorporation affected the microstructure of the BNC. Zaborowska and co-workers (2010) showed that microporous of pure BNC scaffolds enhance the capacity to guide bone tissue formation when cultured with MC3T3-E1 cells.

In current work, the microstructure incorporated with BG might improve even more osteoblasts proliferation, and support new tissue formation.

4.1.1 Mechanical properties

In order to investigate the mechanical properties of BNC and BNC-BG membranes, samples were submitted to tensile strength analyses. Tensile strain, Young modulus and deformation are shown in Table 5.

Table 5 – Mechanical properties of pure BNC and BNC-BG composites.

Sample	Tensile strength (MPa)	Young's modulus (kPa)	Elongation (%)
BNC	0.428 □ 0.074	63.010 □ 8.670	6.787 □ 0.464
BNC-BG	0.885 □ 0.234	180.480 □ 17.240	6.595 □ 1.839

The mechanical behavior of the produced scaffolds shows that Young's modulus and tensile strength increased 186% and 107%, respectively, after BG incorporation were observed into BNC matrix.

No significant difference ($p < 0.05$) as percentage elongation of the samples. SASKA et al. (2011) showed that Young's modulus and strength were also improved compared to BNC alone, when incorporated with silica.

This BNC-BG composite may be suitable for bone repair in places with no load, as in some bones of the face and skull.

Characteristic tensile stress-strain curves for BNC and BNC-BG scaffolds are shown in Figure 23. In the case of BNC samples, the increase of load did not exhibit any pop-in peaks and oriented and unique fracture occurs. On the other hand, BNC-BG shows several fractures until the complete drop of load (Figure 23-a). At first peak, partial and isolate fracture of the membrane occurs, but fibers without damage still remain and the load can be again increased until the complete rupture, in the second highest peak (Figure 24). This behavior could be imputed to the BG particles intertwined with the cellulose nanofibers, which seems to be a reinforcing agent, responsible for the further increase of the mechanical strength of BNC-BG composites.

Figure 23 – Characteristic stress–strain curves from tensile test for BNC and BNC-BG scaffolds (a). Average tensile strength values of each set of samples with elongation percentage are summarized (b).

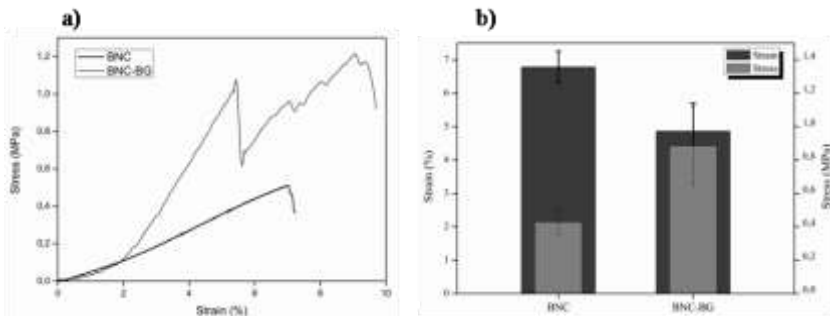
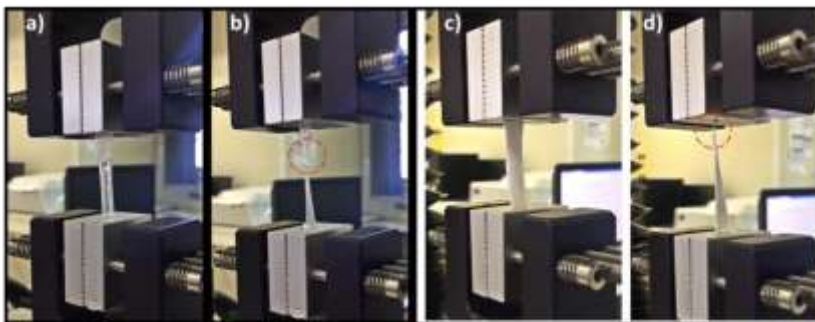


Figure 24 – Fracture strength images for BNC and BNC-BG obtained for loading in tension.

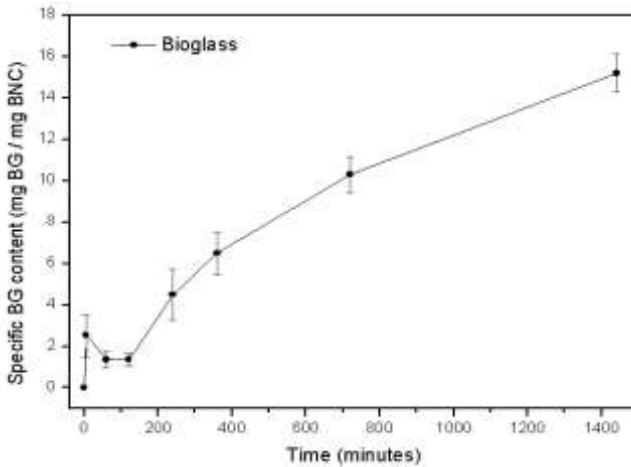


4.2.6 Incorporation Kinetics of Bioglass[®] into BNC matrix

In order to evaluate the fraction of BG incorporated into BNC hydrogel by *ex situ* modification method, initially proposed, pre-synthesized BNC scaffolds were soaked into water which contained BG particles (1% w/v). After predetermined times, BNC-BG composites were removed in triplicate from the solution and freeze-dried. The mass of BG in the BNC matrix was determined by subtracting the total composite weight from the average weight of control nanocellulose membranes.

The change of the cumulative incorporation of BG particles in the membranes, with time, is shown in Figure 25. Results revealed that BG content was increased in the hydrogels with time. Moreover, its incorporation rate could be predicted, indicating the possibility to engineer composites with specific concentration that specific cells need.

Figure 25 BNC-BG incorporation profile when soaked in water solution with BG 1 % (w/v).



BG weight percentages were calculated by dividing the mass of the BG by the total composite weight. At the first 120 minutes, it was estimated 66% of BG in the BNC-BG composite; compare to nearly 93% of BG after 1.440 minutes (1 day) of synthesis.

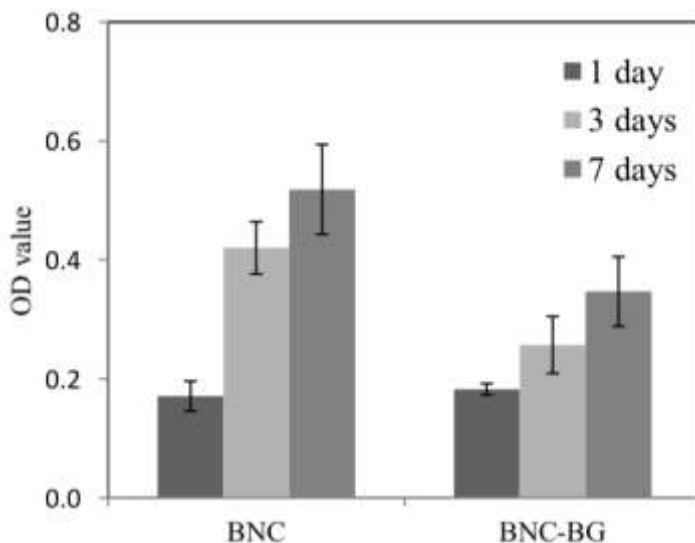
4.3 IN VITRO TESTS

4.3.1 Proliferation of L929 fibroblasts

Most studies with 45S5 bioactive glass evaluate its effects on hard tissue engineering and bone regeneration, analyzing the behavior of osteoblastic cells (HENCH, 1998, 2001). Beyond the evidences of bone stimulation, researches have recently investigated interactions and effects of fibroblast and endothelial cells for soft tissue engineering. Bioactive glass dissolutions products stimulate the expression and secretion of vascular endothelial growth factor from fibroblasts, and subsequently provoke angiogenesis (LEU; LEACH, 2008; LI et al.; 2013; Li et al., 2014) showing a potential for neovascularization of tissue-engineered scaffolds (BALASUBRAMANIAN et al., 2018). Several studies have shown the response of these cells to fixed concentrations of ions released from bioactive glass, without the biomaterial interactions (LI; CHANG, 2013).

The strategy of this work was to evaluate the proliferation of L929 fibroblast seeded onto BNC and BNC-BG composite scaffolds. Cell proliferation analyses were performed at different time points over a period of one week. Results presented in Figure 26 showed that cell proliferation gradually increased over time, suggesting that both scaffolds supported L929 fibroblasts proliferation, as determined by an increase in optical density of MTS assay. Significant differences ($p < 0.05$) were observed between cell proliferation on BNC-BG scaffolds and positive control, pure BNC, after 3 and 7 days. Direct contact of L929 cells showed that proliferation on BNC-BG composite decreased compared to unmodified BNC.

Figure 26 - Cell proliferation assays on BNC scaffolds with or without bioactive glass additions.

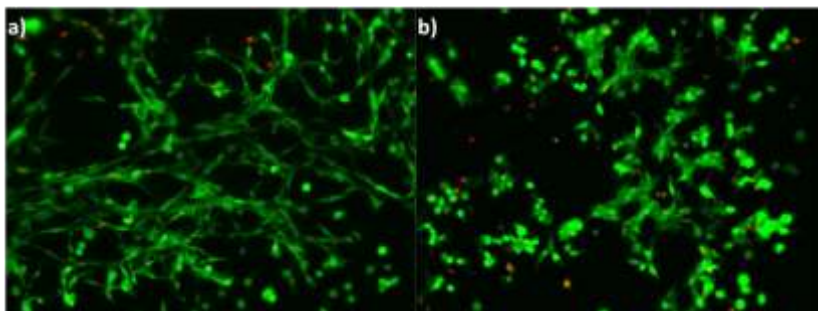


According to ISO 10993-5 (2009), that describes test methods to assess the *in vitro* cytotoxicity of medical devices, BNC-BG composites present cytotoxicity when compared with BNC hydrogels; that means the metabolic activity of L929 fibroblasts is lower than 70% in the material incorporated with BG particles, when associated with metabolic activity in BNC, determined as 100%. The cytotoxicity could be associated with micro-environment changes, alkalization of the

medium and high concentration of bioglass incorporated in the composite (DAY et al., 2005; LI; CHANG, 2013).

Live/Dead® assay was used to evaluate fibroblasts morphology and viability after 7 days of cell seeding. Cells were seeded on the scaffolds as described before, and incubated at 37 °C and 5% CO₂. On each material, adherent cells were observed (Figure 27), showing fibroblast- like morphology (stretched) on BNC hydrogel s(Fig. 27-a) and, on the other hand, rounded morphology observed on the BNC-BG composite (Figure 27-b). This result indicates that the reason of lower proliferation over time, may be associated with the sensitivity of the cells to either the increased of ion dissolution products or the increased pH (DAY, 2005).

Figure 27 – L929 cells after 7 days cultured in BNC (a) and BNC-BG (b) hydrogels. Live cells (green) are distinguished from dead cells (red).



Similar behaviors were also reported by Day (2005), in the case of fibroblasts. CCD- 18C proliferation were tested in plates coated with different amounts of 45S5 Bioglass® (from 0.03125 to 6,25 mg·cm⁻²). After 72h of culture, a significant decrease of metabolically active cells occurred in all concentrations of BG particles; in higher concentrations, it reduced since the first 24 hours. In spite of decreased cell viability, fibroblasts continued to secrete angiogenic growth factors when in BG contact, indicating that VEGF is not connected with cell proliferation. In a similar experimental setting, Day et al. (2004) studied wide range concentrations of BG and their effect on fibroblasts (208F); significant inhibition of cell proliferation occurred with concentrations higher than 0.625 mg/cm² of BG particles compared with untreated control surfaces. It is not seen as a problem that 45S5 bioglass reduce fibroblast proliferation, because the goal for tissue engineering it to get

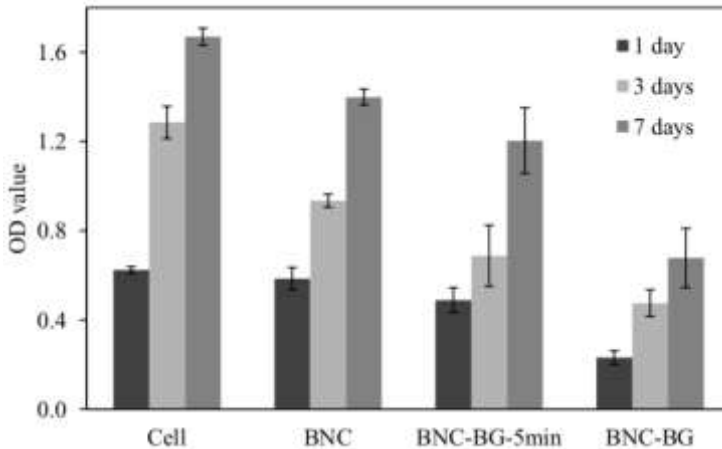
blood vessels to the 3D scaffold, a process that could be impaired if the composite induces fibroblast viability.

Keshaw, Forbes and Day (2005) also assess the number of metabolically active cells encapsulated in alginate spheres containing 45S5 bioactive glass (0.01, 0.1 and 1 % w/v); CCD-18Co fibroblasts cultured indicated no increase in the number of metabolically active cells inside the alginate beads during the study period. With a bigger amount of BG, more reduction was seen in the number of cells, but it did not affect the increase of VEGF secretion.

Alcaide et al. (2010) also used murine L929 fibroblast to evaluate the effect of ordered mesoporous 85SiO₂-10CaO-5P₂O₅ (mol%) bioactive glass in cell proliferation. A significant decrease in cell number was observed after 1 and 7 days culture in the presence of 1% MBG85 powder. Li and Chang (2013) investigated a silicate containing only Si and Ca which were tested on fibroblast cells. It has been determined that silicate extracts at dilutions of 1/16 and 1/32 (1.25 and 0.625% w/v, respectively) reduced the total number of human dermal fibroblasts (HDF) compared with control medium after 48 hours.

In order to explore lower contents of BG in BNC hydrogels, a similar approach was evaluated in this work. *In vitro* cytocompatibility tests were performed with hydrogels containing approximately 1 mg·cm⁻² of bioglass particles, compared to 7.5 mg·cm⁻² from BNC-BG. The concentration of 1 mg·cm⁻² of BG were obtained after 5 minutes of BNC *ex situ* incorporation (BNC-BG-5min). In this *in vitro* test, fibroblasts were seeded into the culture plate during 1 day, then the scaffolds added into each well. After 1, 3 and 7 days of *in vitro* culture, proliferation of L929 cells were determined by MTS. The results confirmed that in higher concentrations of BG particles, the proliferation reduced significantly ($p < 0.05$) since the first day; however, comparing BNC and BNC-BG-5min (1 mg·cm⁻²), the reduction was not significant ($p < 0.05$), which is a good indication of a probable non-cytotoxic composite based on bacterial nanocellulose and Bioglass®, revealing a candidate material for soft-tissue engineering scaffolds.

Figure 28 - Cell proliferation assays on pure BNC scaffolds and BNC-BG with different contents of BG particles.



The current study focused on the development of a BNC-BG composite material for hard tissue engineering; however, even if fibroblastic cell inhibition occurs, this fact may be beneficial, because if fibroblasts overgrowth, it could inhibit the growth of other cell types, such as endothelial cells or osteoblasts, than preclude the use of this material in other tissues.

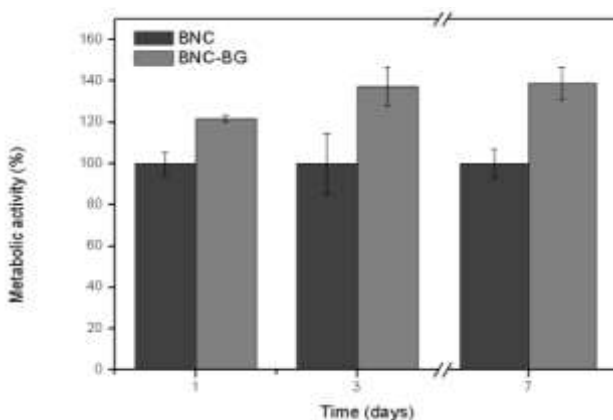
4.3.2 Metabolic activity of MC3T3-E1 on BNC and BNC-BG hydrogels

The interactions between scaffolds and cells are crucial for the future design of improved biomaterials. Osteoblasts are the main, calcified matrix-secreting cell type in bone and its evaluation and proliferation are important in hard tissue engineering. Dissolution products from 45S5 Bioglass® have also been shown to induce osteoblastic differentiation and proliferation (REILLY et al., 2007; SHANKHWAR; SRINIVASAN, 2016). MC3T3-E1 cell line has the capacity to differentiate into osteoblasts and osteocytes and have been demonstrated to form calcified bone tissue *in vitro* (LAZARY et al., 2008). Zimmermann et al. (2011) asserted that osteoprogenitor cells

(MC3T3-E1) differentiated to osteoblasts after 12 days cultured in a composite based on BNC incorporated with HA.

Pre-osteoblasts (MC3T3-E1) response after *in vitro* culture on BNC, and BNC-BG composites are showed at Figure 29. The influence of BG showed increased metabolic activities on the composites when compared to unmodified membrane (control), suggesting a proliferative potential of the BNC-BG material. The metabolic activity of MC3T3-E1 cells cultured by direct contact with BNC-BG hydrogels were 122% (1 day), 137% (3 days) and 139% (7 days) compared to BNC hydrogels (100%).

Figure 29 – Metabolic activity of osteoblasts cells.



The presence of calcium and phosphate from HA in BNC membranes promotes osteoblast cell adhesion and growth (SASKA et al.,2011; STROBEL et al., 2012;TAZI et al., 2012). This hypothesis is supported by results obtained with 45S5 bioactive glass, indicating that BNC-BG composites are biocompatible and a potential scaffold material for hard tissue engineering.

Significant differences were observed when compared the metabolic activity of pre- osteoblasts cells cultured in contact with BNC and BNC–BG hydrogels. The positive effect of Bioglass on polymer composite tested in MC3T3-E1 cell proliferation confirms the novel material a good candidate scaffold for advanced bone tissue engineering.

5 CONCLUSIONS

A novel biocomposite based on bacterial nanocellulose and Bioglass® was successfully produced by the *ex situ* process. The synthesis in a solution containing water provided the best incorporation, where BG particles were homogeneously integrated among the nanofibers of the polymer. The BNC matrix arranged the desired bonding for BG particles, which provided a great surface area to mineralize HA and improve young's modulus and mechanical strength of the composites.

This work also aimed to analyze the cellular response in the composites for tissue regeneration. *In vitro* culture showed that low concentration of BG in BNC matrix favored the proliferation of fibroblasts when compared with larger amounts; and showed no significant difference with pure BNC. The metabolic activity analysis of preosteoblasts seeded on the scaffolds demonstrated a higher attachment and proliferation on BNC-BG composites throughout the experiment, presenting good biocompatibility and potential biomaterial for hard tissue regeneration.

Bioactive glass particles encapsulated by the BNC matrix can effectively regulate the physiological activity of different cell lines. The rate of incorporation of BG can be predicted, indicating the possibility of designing compounds with specific concentration that specific cells need. This implies that BNC-Bioglass® hydrogels can notably distinguish their use in soft- tissue and hard-tissue engineering and suggests potential advanced use as biomaterial for bone regeneration.

5.1 SUGGESTED FUTURE WORKS

- Investigate the excretion of VEGF and *in vitro* response of endothelial cells;
- Analyze the differentiation of the MC3T3-E1 preosteoblasts into osteoblasts.
- Evaluate a co-cultured of L929 and MC3T3-E1.
- Evaluate the biomaterial *in vivo*.
- Quantification of Ca and Si.

REFERENCES

- ALCAIDE, M.; PORTOLES, P.; LOPEZ-NORIEGA, A.; ARCOS, D.; VALLET-REGI, M.;
- PORTOLES, M.T. **Interaction of an ordered mesoporous bioactive glass with osteoblasts, fibroblasts and lymphocytes, demonstrating its biocompatibility as a potential bone graft material.** *Acta Biomaterialia*, v.;6, p. 892–899, 2010.
- ALMEIDA, I. F.; PEREIRA, T.; SILVA, N. H. C. S.; GOMES, F. P.; SILVESTRE, A. J. D.,
- FREIRE, C. S. R., SOUSA LOBO J. M.; COSTA P. C. **Bacterial cellulose membranes as drug delivery systems: an in vivo skin compatibility study.** *European Journal of Pharmaceutics and Biopharmaceutics*, v.86, p.332-336, 2014.
- ASHORI, A.; SHEYKHNAZARI, S.; TABARSA, T.; SHAKERI, A.; GOLALIPOUR, M.
- Bacterial cellulose/silica nanocomposites: Preparation and characterization.** *Carbohydrate Polymers*, p. 413–418, 2012.
- ATWOOD, R. C.; BODEY, A. J.; PRICE, S. W. T.; BASHAM, M.; DRAKOPOULOS, M. A
- high-throughput system for high-quality tomographic reconstruction of large datasets at Diamond Light Source.** *Philosophical Transactions of the Royal Society A: Mathematical, Physical and Engineering Sciences*, v. 373, p. 398, 2015.
- BAINO, F.; HAMZEHLU, S.; KARGOZAR, S. **Bioactive Glasses: Where Are We and Where Are We Going?** *Journal of Functional Biomaterials*, v. 9, p.25, 2018.
- BAKER, S. C.; ROHMAN, G. R.; SOUTHGATE, J.; CAMERON, N. R., **The relationship between the mechanical properties and cell behavior on PLGA and PCL scaffolds for bladder tissue engineering.** *Biomaterials*, v. 30, p. 1321-1328, 2009.
- BALASUBRAMANIAN, P.; BÜTTNER, T.; PACHECO, V. M.; BOCCACCINI, A.R. **Boron-containing bioactive glasses in bone and soft tissue engineering.** *Journal of the European Ceramic Society*, v. 38, p. 855-869, 2018.
- BARUD, H. G.; SILVA, R. R.; BARUD, H.; TERCJAK, A.; GUTIERREZ, J.; LUSTRI, W. R.;

RIBEIRO, S. J. L. **A multipurpose natural and renewable polymer in medical applications: Bacterial cellulose.** Carbohydrate Polymers, v.153, p. 406–420, 2016.

BOCCACCINI, A.R.; BLAKER, J.J.; MAQUET, V.; DAY, R.M.; JEROME, R.; **Preparation and characterization of poly(lactide-co-glycolide) (PLGA) and PLGA/Bioglass(R) composite tubular foam scaffolds for tissue engineering applications.** Materials Science and Engineering: C, p. 25-31, 2005.

BOCCACCINI, A.R.; MAQUET, V. **Bioresorbable and bioactive polymer/ Bioglass(R) composites with tailored pore structure for tissue engineering applications.** Composites Science and Technology, p. 2417-2429, 2003.

CACICEDO, M.L.; LEÓN, I.E.; GONZALEZ, J.S.; PORTO, L. M.; ALVAREZ, A.; VERA ; C.,

GUILLERMO, R. **Modified bacterial cellulose scaffolds for localized doxorubicin release in human colorectal HT-29 cells.** Colloids and Surfaces -biointerfaces, v. 140, p. 421-429, 2016.

CASTRO, C.; ZULUAGA, R.; PUTAUX, J.-L.; CARO, G.; MONDRAGON, I.; GAÑÁN, P.

Structural characterization of bacterial cellulose produced by Gluconacetobacterswingsii sp. from Colombian agroindustrial wastes. Carbohydrate Polymers, v. 84, n. 1, p. 96-102, 2011.

CHAN, B.; LEONG, K. **Scaffolding in tissue engineering: general approaches and tissue- specific considerations,** European Spine Journal., v. 17, p. 467–479, 2008.

CHEN, Q.; BAINO, F.; SPRIANO, S.; PUGNO, N.M.; VITALE-BROVARONE, C. **Modelling**

of the strength– porosity relationship in glass-ceramic foam scaffolds for bone repair. Journal of the European Ceramic Society, v.34, p. 2663-2673, 2014.

CHEN, Q.Z.; THOMPSON, I.D.; BOCCACCINI, A.R. **45S5 Bioglass®-derived glass-ceramic scaffolds for bone tissue engineering.**Biomaterials, p. 2414-2425, 2006.

CHEN, Y.W.; CHIOU, S.H.; WONG, T.T.; KU, H.H.; LIN, H.T.; CHUNG, C.F.; YEN, S.H.;

KAO, CL. **Using gelatin scaffold with coated basic fibroblast growth factor as a transfer system for transplantation of human neural stem cells.**Transplantation Proceedings, v.38, p. 1616-1617, 2006.

COLLA, G. **Desenvolvimento de um reator biológico tecidual muscular a partir de vasos de celulose bacteriana.** Dissertação, Engenharia Química da Universidade Federal de Santa Catarina. Florianópolis, 2014.

CZAJA, W. K.; YOUNG, D. J.; KAWECKI, M.; BROWN, R. M. **The Future Prospects of microbial cellulose in biomedical Applications.** *Biomacromolecules*, v.8, n.1, p.1-12, 2007.

DAY, R. M. **Bioactive Glass Stimulates the Secretion of Angiogenic Growth Factors and Angiogenesis *in vitro*.** *Tissue engineering*, v.11, 2005.

DAY, R.M.; BOCCACCINI, A.R.; SHUREY, S.; ROETHER, J.A.; FORBES, A.; HENCH, L.L.

Assessment of polyglycolic acid mesh and bioactive glass for soft-tissue engineering scaffolds. *Biomaterials*, p. 5857-5866, 2004.

DAY, R.M.; MAQUET, V.; BOCCACCINI, A. R.; JÉRÔME, R.; FORBES, A. ***In vitro* and in**

vivo analysis of macroporous biodegradable poly(D,L-lactide-co-glycolide) scaffolds containing bioactive glass. *Journal of Biomedical Materials Research - Part A*, v.75, p. 778-787, 2005.

DELIORMANLI, A.M. **Investigation of *in vitro* mineralization of silicate-based 45S5 and 13- 93 bioactive glasses in artificial saliva for dental applications.** *Ceramics International*, v.43, p. 3531–3539, 2017.

DENG, H.W.; LIU, Y.Z. **Current topics in bone biology.** *World Scientific*, p. 230-254, 2005.

DOULABI, A. H.; MEQUANINT, K.; MOHAMMADI, H. **Blends and Nanocomposite Biomaterials for Articular Cartilage Tissue Engineering.** *Materials*, v. 7, p. 5327-5355, 2014.

DU, J.; XIANG, Y. **Effect of strontium substitution on the structure, ionic diffusion and dynamic properties of 45S5 Bioactive glasses.** *Journal of Non-Crystalline Solids*, v. 358, p. 1059-1071, 2012.

EQTESADI, S.; MOTEALLEH, A.; PERERA, F. H.; PAJARES, A.; MIRANDA, P. **Poly-**

(lactic acid) in filtration of 45S5 Bioglassrobocast scaffolds: Chemical interaction and its deleterious effect in mechanical enhancement. *Materials Letters*, v.163, p. 196-200, 2016.

EROL, M. M.; MOURINO, V.; NEWBY, P.; CHATZISTAVROU, X.; ROETHER, J. A.;

HUPA, L.; BOCCACCINI, A.R. **Copper-releasing, boron-containing bioactive glass-based scaffolds coated with alginate for bone tissue engineering.** *Acta Biomaterialia*, v. 8, p. 792–801, 2012.

FENG Y.; ZHANG X.; SHEN Y.; YOSHINO K.; FENG W. **A mechanically strong, flexible and conductive film based on bacterial cellulose/graphene nanocomposite.** *Carbohydrate Polymers*, v. 87, p. 644–649, 2012.

FU, L.; ZHANG, J.; YANG, G. **Present status and applications of bacterial cellulose-based materials for skin tissue repair.** *Carbohydrate Polymers*, p.1432–1442, 2013.

GERHARDT, L.C.; BOCCACCINI, A.R. **Bioactive glass and glass-ceramic scaffolds for bone tissue engineering.** *Materials*, v. 3, p. 3867, 2010.

GODINHO, J. F.; BERTI, F. V.; MULLER, D.; RAMBO, C. R.; PORTO, L. M. **Incorporation of Aloe vera extracts into nanocellulose during biosynthesis.** *Cellulose*, v. 23, p. 545-555, 2016.

GORUSTOVICH, A.A.; ROETHER, J.A.; BOCCACCINI, A. R. **Effect of Bioactive Glasses on Angiogenesis: A Review of *In vitro* and In Vivo Evidences,** *Tissue Engineering Part B Reviews*, v. 16, p. 199-207, 2010.

GRANDE, C. J.; TORRES, F. G.; GOMEZ, C. M.; CARMEN BAÑÓ, M. **Nanocomposites of bacterial cellulose/hydroxyapatite for biomedical applications.** *Acta Biomaterialia*, v. 5, p. 1605–1615, 2009.

GRIFFITH, L.; NAUGHTON, G. **Tissue Engineering—Current Challenges and Expanding Opportunities.** *Science*, v. 295, n.5557, p. 1009-1014, 2002.

GUNAWIDJAJA, P. N.; MATHEW, R.; LO, A. Y. H.; IZQUIERDO-BARBA, I.; GARCIA, A.;

ARCOS, D.; EDEN, M. **Local structures of mesoporous bioactive glasses and their surface alterations *in vitro*: inferences from solid-state nuclear magnetic resonance.** *Philosophical Transactions of the Royal Society A: Mathematical, Physical and Engineering Sciences*, p. 1376- 1399, 2012.

HASAN, A.; RAGAERT, K.; SWIESZKOWSKI, W.; SELIMOVIC, S.; PAUL, A.; CAMCI-

UNAL, G. **Biomechanical properties of native and tissue engineered heart valve constructs.** Journal of Biomechanics, v. 47, p. 1949–1963, 2014.

HASAN, M. S.; WERNER-ZWANZIGER, U.; BOYD, D. **Composition-structure-properties relationship of strontium borate glasses for medical applications.** Journal of Biomedical Materials Research - Part A, v. 103, p. 2344–2354, 2015.

HENCH, L. L. **Biomaterials: A forecast for the future.** Biomaterials, v. 19, p. 1419–1423, 1998.

HENCH, L.L. **Bioceramics.** Journal of the American Ceramic Society, p.1705–1728,1998;

HENCH, L.L. **Opening paper 2015 - some comments on bioglass: four eras of discovery and development.** Biomedical Glasses, p. 1–11, 2015.

HENCH, L.L., **Genetic design of bioactive glass.** Journal of the American Ceramic Society, v. 29, p. 1257–1265, 2009.

HENCH, L.L.; DAY, D.E.; HOLAND, W.; RHEINBERGER, V.M. **Glass and medicine,** International Journal of Applied Glass Science, v.1, p. 104–117, 2010.

HENCH, L.L.; POLAK, J.M. **Third-generation biomedical materials.** Science; v. 295, p. 1014–1017. 2002.

HENCH, L.L.; SPLINTER, R.J.; ALLEN, W.C.; GREENLEE, T.K. **Bonding mechanisms at the interface of ceramic prosthetic materials.** Biomedical Materials Research, v.5, p. 117–141, 1971.

HENRIQUE, J.; MARIA, E.; FONSECA, B.; MAZALI, I. O.; MAGALHÃES, A.; LANDERS, R.; APARECIDO, C. **Facile and innovative method for bioglass surface modification: Optimization studies.** Materials Science and Engineering C, v.72, p. 86–97, 2017.

HONG,L.;WANG,Y.L.;JIA,S.R.;HUANG,Y.;GAO,C.;WAN,Y.Z.

Hydroxyapatite/bacterial cellulose composites synthesized via a biomimetic route. Materials Letters, p. 1710–1713, 2006.

HONGLIN, L.; DEHUI, J.; WEI, L.; JIAN, X.; CHUNZHI, L.; GUANGYAO, X.; YONG, Z.;

YIZAO, W. **Constructing a highly bioactive 3D nanofibrousbioglass scaffold via bacterial cellulose-templated sol-gel approach.** Materials Chemistry and Physics. p. 176, 2016.

HOPPE, A., GULDAL, N.S.; BOCCAACCINI, A.R. **A review of the biological response to ionic dissolution products from bioactive glasses and glass-ceramics.** Biomaterials, v. 32, p. 2757-2774, 2011.

HORCH, R.E.; KNESER, U.; POLYKANDRIOTIS, E.; SCHMIDT, V.; SUN, J. **Tissue**

engineering and regenerative medicine – where do we stand ? Journal of Cellular and Molecular Medicine, v. 6, p. 1157-1165, 2012.

HUANG, X.; YANG, D.; YAN, W.; SHI, Z.; FENG, J.; GAO, Y.; WENG, W.; YAN, S.

Osteochondral repair using the combination of fibroblast growth factor and amorphous calcium phosphate/poly(L-lactic acid) hybrid materials. Biomaterials, v. 28, p.3091–3100, 2007.

INTERNATIONAL ORGANIZATION FOR STANDARDIZATION. **ISO 10993–5**, Biological

Evaluation of Medical Devices -Tests for *In vitro* Cytotoxicity, v. 5, p. 1-52, 2009.

JONES, J. R. **Review of Bioactive Glass: From Hench to Hybrids.** Acta Biomaterialia, v. 9, p. 4457-4486, 2013.

JONES, J.R.; BRAUER, D.S.; HUPA, L.; GREENSPAN, D.C. **Bioglass and bioactive glasses and their impact on healthcare.** International Journal of Applied Glass Science., v.7, p. 423– 434, 2016.

JOZALA, A.F.; LENCASTRE-NOVAES, L.C; LOPES, A.M.; SANTOS-EBINUMA V.D.; MAZZOLA, P.G.; PESSOA, A.; GROTO D.; GERENUTTI, M.; CHAUD, M.V. **Bacterial**

nanocellulose production and application: a 10-year overview. Applied Microbiology and Biotechnology, p. 2063–2072, 2016.

JUNG, S.; DAY, D.; DAY, T.; STOECKER, W.; TAYLOR, P. **Treatment of non-healing diabetic venous stasis ulcers with bioactive glass nanofibers.** Wound Repair and Regeneration, p.19-30, 2011.

KACPERSKA, A. **Solubilities of Sodium and Potassium Iodides in Water- n -Propyl Alcohol Mixtures at 25°C.** Physics and Chemistry of Liquids, v. 26, p. 273–280, 1994.

KARAGEORGIU, V.; KAPLAN, D. **Porosity of 3D biomaterial scaffolds and osteogenesis.** Biomaterials, v. 26, p. 5474-5491, 2005.

KAULLY, T.; KAUFMAN-FRANCIS, K.; LESMAN, A.; LEVENBERG, S. **Vascularization-**

the conduit to viable engineered tissues. Tissue Engineering, Part B, p. 159, 2009.

KESHAW, H.; FORBES, A.; DAY, R.M. **Release of angiogenic growth factors from cells encapsulated in alginate beads with bioactive glass.** Biomaterials, v.26, p. 4171–4179, 2005.

KESKIN, Z.; SENDEMIR URKMEZ, A.; HAMES, E. **Novel keratin modified bacterial cellulose nanocomposite production and characterization for skin tissue engineering.** Material Science and Engineering, v.75, p. 1144-1153, 2017.

KLEMM, D.; SCHUMANN, D.; UDHARDT, U.; MARSCH, S. **Bacterial synthesized cellulose-artificial blood vessels for microsurgery.** Progress in Polymer Science, v. 26, p. 1561– 1603, 2001.

KOKUBO, T.; KUSHITANI, H.; SAKKA, S.; KITSUGI, T.; YAMAMURO, T. **Solutions able**

to reproduce in vivo surface-structure changes in bioactive glass-ceramic A-W. Journal of Biomedical Materials Research, v.24, p. 721–734, 1990.

KOKUBO, T.; TAKADAMA, H. **How useful is SBF in predicting in vivo bone bioactivity?** Biomaterials, v. 27, p. 2907–2915, 2006.

KUMAR, A.; RAO, K. M.; KWON, S. E.; LEE, Y. N.; HAN, S. S. **Xanthan gum/bioactive**

silica glass hybrid scaffolds reinforced with cellulose nanocrystals: Morphological, mechanical and *in vitro* cytocompatibility study. Materials Letters, v. 193, p. 274–278, 2017.

LANGER, R.; VACANTI J. P. **Tissue engineering.** Science, v. 260, p. 920–925, 1993.

LANZA, R.; LANGER, R.; VACANTI, J. P. **Principles of tissue engineering.** Academic press, 2011.

LAZÁRY, A.; BALLA, B.; J.P. KÓSA, K. BÁCSI, Z. NAGY, I. TAKÁCS, P.P. VARGA,

G.; SPEERLAKATO, P. **Effect of gypsum on proliferation and differentiation of MC3T3-E1 mouse osteoblastic cells.** Biomaterials, v. 28 p. 393–399, 2008.

LEGEROS R. Z. **Properties of osteoconductive biomaterials: Calcium phosphates.** Clinical Orthopaedics and Related Research, v. 395, p. 81–98, 2002.

LEU, A.; LEACH, J. K., **Proangiogenic potential of a collagen/bioactive glass substrate.** Pharmaceutical Research, v. 25, p.1222–1229, 2008.

LI, H.; CHANG, J. **Bioactive silicate materials stimulate angiogenesis in fibroblast and endothelial cell co-culture system through paracrine effect.** *Acta Biomaterialia*, v.9, p. 6981– 6991, 2013.

LI, W.; NOOEAD, P.; ROETHER, J. A.; SCHUBERT, D. W.; BOCCACCINI, A. R.

Preparation and characterization of vancomycin releasing PHBV coated 45S5 Bioglass®- based glass-ceramic scaffolds for bone tissue engineering. *Journal of the European Ceramic Society*, v. 34, p. 505–514, 2014.

LIEN, S.M.; KO, L.Y.; HUANG, T.J. **Effect of crosslinking temperature on compression strength of gelatin scaffold for articular cartilage tissue engineering.** *Materials Science and Engineering*, v.30, p. 631-635, 2010.

LIU, X.; RAHAMAN, M.N.; DAY, D.E. **Conversion of melt derived microfibrinous borate (13- 93B3) and silicate (45S5) bioactive glass in simulated body fluid.** *Journal of Materials Science: Materials in Medicine*, v.24, p. 583-595, 2013.

LOVETT, M.; LEE, K.; EDWARDS, A.; KAPLAN, D.L. **Vascularization strategies for tissue engineering.** *Tissue Engineering-Part B*, v. 15, p. 353, 2009.

LU, H.H.; TANG, A.; OH, S.C.; SPALAZZI, J.P.; DIONISIO, K. **Compositional effects on the formation of a calcium phosphate layer and the response of osteoblast-like cells on polymer- bioactive glass composites.** *Biomaterials*; v. 26, p. 6323-6334, 2005.

MAQUET, V.; BOCCACCINI, A. R.; PRAVATA, L.; NOTINGHER, I.; JÉRÔME, R. **Porous poly(α -hydroxyacid)/Bioglass® composite scaffolds for bone tissue engineering. I: preparation and *in vitro* characterisation.** *Biomaterials*, v. 25, n. 18, p. 4185-4194, 2004.

MCMANUS, A.J.; DOREMUS, R.H.; SIEGEL, R.W.; BIZIOS, R. **Evaluation of cytocompatibility and bending modulus of nanoceramic/polymer composite.** *J Biomed Materials*, v. 72, p. 98-106, 2005.

NGUYEN, V. T., GIDLEY, M. G., & DYKES, G. A. **Potential of a nisin-containing bacterial cellulose film to inhibit *Listeria monocytogenes* on processed meats.** *Food Microbiology*, v. 25, p. 471–478, 2008.

NIBIB. **National Institutes of Health- Biomaterials.** United States, Sep., 2017.

- NIMESKERN, L.; MARTÍNEZ A. H.; SUNDBERG, J.; GATENHOLM, P.; MÜLLER, R.; STOK, K. **Mechanical evaluation of bacterial nanocellulose as an implant material for ear cartilage replacement.** Mechanical behavior of biomedical materials, v. 22, p. 11-21, 2013.
- OHGUSHI, H.; ISHIMURA, M.; HABATA, T.; TAMAI, S. **Porous ceramics for intra- articular depression fracture, Biomaterials and bioengineering handbook.**, Marcel Dekker, New York, p. 397-405, 2000.
- OONISHI, H.; HENCH, L. L.; WILSON, J.; SUGINARA, F.; TSUJI, E.; KUSHITANI, S.;
- WAKI, H. **Comparative bone growth behavior in granules of bioceramic materials of various sizes.** Journal of Biomedical Materials Research, v. 44, p. 31–43, 1999.
- OUADESSE, H.; BUI, X.V.; GAL, Y. L.; MOSTAFA, A.; CATHELINÉAU, G. **Chitosan Effects on Bioactive Glass for Application as Biocomposite Biomaterial.** International Journal of Biology and Biomedical , v. 5, p. 49–56, 2011.
- OUADESSE, H.; DIETRICH, E.; GAL, Y.L.; PELLEN, P.; BUREAU, B.; MOSTAFA, A.A.;
- CATHELINÉAU, G. **Apatite forming ability and cytocompatibility of pure and Zn-doped bioactive glasses.** Biomedical Materials, 2011.
- PALSSON, B.O.; BHATIA, S.N. **Tissue engineering.** London: Pearson Educatio, 2004.
- PERTILE, R.; MOREIRA, S.; ANDRADE, F.; DOMINGUES, L.; GAMA, M. **Bacterial cellulose modified using recombinant proteins to improve neuronal and mesenchymal cell adhesion.** Biotechnology Progress, v.28, p.526-532, 2012.
- PERTILE, R.A.N.; MOREIRA, S.; GIL DA COSTA, R.M.; CORREIA, A.; GUARDAO, L.;
- GARTNER, F.; VILANOVA, M.; GAMA, M. **Bacterial cellulose: long-term biocompatibility studies.** Biomaterials Science and Polymers. v. 23, p. 1339-1354, 2012.
- PETER, M.; BINULAL, N.S.; NAIR, S.V.; SELVAMURUGAN, N.;
- TAMURAH.;
- JAYAKUMAR, R. **Novel biodegradable chitosan-gelatin/nano-bioactive glass ceramic composite scaffolds for alveolar bone tissue engineering.** Chemical Engineering, v. 153, p. 353–361, 2010.

PITELLA, C.Q.P. Desenvolvimento de scaffolds de nanocelulose bacteriana com modificações para aplicações tópicas. Tese em Engenharia Química. Universidade Federal de Santa Catarina. Florianópolis, p. 144, 2017.

PITTELLA, C.Q.P. **Desenvolvimento de scaffold de nanocelulose bacteriana com modificação de superfície para aplicações tópicas.** Tese (doutorado) em Engenharia Química. Universidade Federal de Santa Catarina, Florianópolis, 2017.

PRADEEP, A.; SHARMA, A. **Comparison of clinical efficacy of a dentifrice containing calcium sodium phosphosilicate to a dentifrice containing potassium nitrate and to a placebo on dentinal hypersensitivity: A randomized clinical trial.** Journal of Periodontology, v.81, p. 1167–1173, 2010.

RAMBO, C. R.; RECOUVREUX, D. O. S.; CARMINATTI, C. A.; PITLOVANCIV, A. K.

Template assisted synthesis of porous nanofibrous cellulose membranes for tissue engineering. Materials Science, v. 28, p. 549–554, 2008.

RAMBO, C.R.; MUELLER, F.A.; MUELLER, L.; SIEBER, H.; HOFMANN, I., GREIL, P.

Biomimetic apatite coating on biomorphous alumina scaffolds. Materials Science and Engineering: C, v.26, p. 92, 2006.

RAN, J.; JIANG, P.; LIU, S.; SUN, G.; YAN, P.; SHEN, X.; TONG, H.

Constructing multi-component organic/inorganic composite bacterial cellulose-gelatin/hydroxyapatite double-network scaffold platform for stem cell-mediated bone tissue engineering. Materials Science and Engineering: C, v. 78, p. 130–140, 2017.

RATNER, B. D.; HOFFMAN, A. S.; SCHOEN, F. J.; LEMONS, J.E.

Biomaterials Science - An

Introduction to Materials in Medicine, Elsevier: Oxford, 2013.

RECOUVREUX, D. O. S. **Desenvolvimento de Novos Biomateriais Baseados em Celulose Bacteriana para Aplicações Biomédicas e de Engenharia de Tecidos.** Tese em Engenharia Química, Universidade Federal de Santa Catarina, Florianópolis, p. 124, 2008.

RECOUVREUX, D. O. S.; RAMBO, C. R.; BERTI, F. V.; CARMINATTI, C. A.; ANTÔNIO,

R. V.; PORTO, L. M. **Novel three-dimensional cocoon-like hydrogels for soft tissue regeneration.** Materials Science and Engineering C, v.31, p. 151–157, 2011.

- REILLY, G.C.; RADIN, S.; CHEN, A.T.; DUCHEYNE, P. **Differential alkaline phosphatase responses of rat and human bone marrow derived mesenchymal stem cells to 45S5 bioactive glass**, *Biomaterials*, v. 28 , p. 4091–4097, 2007.
- REIS, E. M.; BERTI, F. V.; COLLA, G.; PORTO, L.M. **Bacterial nanocellulose-IKVAV hydrogel matrix modulates melanoma tumor cell adhesion and proliferation and induces vasculogenic mimicry *in vitro***. *Journal of biomedical materials research part b*, v. 1, p. 1, 2017.
- REZWAN, K.; CHEN, Q. Z.; BLAKER, J. J.; ROBERTO, A. **Biodegradable and bioactive porous polymer / inorganic composite scaffolds for bone tissue engineering**. *Biomaterials*, v. 27, p. 3413–3431, 2006.
- RICHARDSON, T. P.; PETERS, M. C.; ENNETT, A. B.; MOONEY, D. J. **Polymeric system for dual growth factor delivery**. *Nature biotechnology*, v. 19, n. 11, p. 1029-1034, 2001.
- ROMEIS, S.; HOPPE, A.; DETSCH, R.; BOCCACCINI, A. R.; SCHMIDT, J.; PEUKERT, W. **Top-down processing of submicron 45S5 Bioglass® for enhanced *in vitro* bioactivity and biocompatibility**. *Procedia Engineering*, v. 103, p. 534-541 , 2015.
- SAL, H.; FU, R.; XIANG, J.; GUAN, Y.; ZHANG, F. **Fabrication of elastic silica-bacterial cellulose composite aerogels with nanoscale interpenetrating network by ultrafast evaporative drying**. *Composites Science and Technology*, v. 155, p. 72-80, 2018.
- SAIBUATONG, O.A.; PHISALAPHONG, M. **Novo Aloe Vera-Bacterial Cellulose Composite Film From Biosynthesis**. *Carbohydrate Polymers*, v.79, p. 455–460, 2010.
- SASKA, S.; BARUD, H.S.; GASPAR, M.M.; MARCHETTO, R.; RIBEIRO, S.J.L.; MESSADDEQ, Y. **Bacterial cellulose–hydroxyapatite nanocomposites for bone regeneration**, *Biomaterials*, 2011 .
- SERPOOSHAN, V.; JULIEN, M.; NGUYEN, O. **Reduced hydraulic permeability of three- dimensional collagen scaffolds attenuates gel contraction and promotes the growth and differentiation of mesenchymal stem cells**. *Actabiomaterialia*, v. 6, p. 3978- 3987, 2010.
- SHANKHWAR, N.; SRINIVASAN, A. **Evaluation of sol-gel basedmagnetic 45S5 bioglass and bioglass-ceramics containing iron oxide**, *Material Science and Engineering. C*, v. 62, p. 190–196, 2016.

- SHI, Z.; ZHANG, Y.; PHILLIPS, G. O.; YANG, G. **Utilization of bacterial cellulose in food.** Food Hydrocolloids, v.35, p. 539–545, 2014.
- SHOICHET, M. S., **Polymer scaffolds for biomaterials applications.** Macromolecules, v. 43, p. 581-591, 2010.
- STROBEL, L.; RATH, S.; MAIER, A.; BEIER, J.; ARKUDAS, A.; GREIL, P.; HORCH, R.; KNESER, U. **Induction of bone formation in biphasic calcium phosphate scaffolds by bone morphogenetic protein-2 and primary osteoblasts.** Tissue Engineering and Regenerative Medicine, v. 8, p. 176-185, 2012.
- STUMPF, T. R., YANG, X., ZHANG, J., & CAO, X. **In situ and ex situ modifications of bacterial cellulose for applications in tissue engineering.** Materials Science and Engineering: C, v. 372-383, 2018.
- STUMPF, T. R.; PÉRTILE, R. A. N.; RAMBO, C. R.; PORTO, L. M. **Enriched glucose and dextrin mannitol-based media modulates fibroblast behavior on bacterial cellulose membranes.** Materials Science and Engineering: C, v. 33, n. 8, p. 4739-4745, 2013.
- TAZI, N.; ZHANG, Z.; MESSADDEQ, Y.; ALMEIDA-LOPES, L.; ZANARDI, L. M.; LEVINSON, D.; ROUABHIA, M. **Hydroxyapatite bioactivated bacterial cellulose promotes osteoblast growth and the formation of bone nodules.** AMB Express, v. 2, p. 1-10. (2012).
- UL-ISLAM, M.; KHAN, T.; PARK, J.K. **Water holding and release properties of bacterial cellulose obtained by *in situ* and *ex situ* modification,** Carbohydrate Polymers. v. 88, p. 596– 603, 2012.
- URBINA, L.; GUARESTI, O.; REQUIES, J.; GABILONDO, N.; ECEIZA, A.; CORCUERA, M.A.; RETEGI, A. **Design of reusable novel membranes based on bacterial cellulose and chitosan for the filtration of copper in wastewaters.** Carbohydrate Polymers, v.193, p. 362- 372, 2018.
- VARGAS, G.E.; VERAMESONES, R.; BRETCANU, O.; PORTOLOPEZ, J.M.; BOCCACCINI, A.R.; GORUSTOVICH, A. **Biocompatibility and bone mineralization potential of 45S5 Bioglass-derived glass–ceramic scaffolds in chick embryos.** ActaBiomaterialia, v. 5, p. 374, 2009.
- WAGONER JOHNSON, A.J.; HERSCHLER, B.A. **A review of the mechanical behavior of CaP and CaP/polymer composites for applications in bone replacement and repair.** ActaBiomaterialia, v. 7, p. 16–30, 2011.

- WEN,C.; HONG, Y.; WU, J.; LUO, L.; QIU, Y.; YE, J.**The facile synthesis and bioactivity of a 3D nanofibrousbioglass scaffold using an amino-modified bacterial cellulose template.** Royal Society of Chemistry, v. 8, p. 14561-14569, 2018.
- WU, S.C.; LIA, Y.K.; HO, C.Y. **Glucoamylase immobilization on bacterial cellulose using periodate oxidation method.** International Journal of Science and Engineering, v. 3, n. 4, p. 1–4, 2013.
- XU, C.; SU, P.; CHEN, X.; MENG, Y.; YU, W.; XIANG, A.P. **Biocompatibility and osteogenesis of biomimetic Bioglass-collagen-phosphatidylserine composite scaffolds for bone tissue engineering.**Biomaterials, v.32, p. 1051-1058, 2011.
- XYNOS, D.; EDGAR, A. J.; BUTTERY, L. D.; HENCH, L. L.; POLAK, J. M. **Gene-expression profiling of human osteoblasts following treatment with the ionic products of Bioglass 45S5 dissolution.**Biomedical Materials, p. 151–157, 2001.
- XYNOS, D.; EDGAR, A. J.; BUTTERY, L. D.; HENCH, L. L.; POLAK, J. M. **Ionic products of bioactive glass dissolution increase proliferation of human osteoblasts and induce insulin- like growth factor II mRNA expression and protein synthesis.** Biochemical and Biophysical Research Communications, p. 461–465, 2000.
- YANG, G.; YANG, X.; ZHANG, L.; LIN. M.; SUN, X.; CHEN, X. **Counterionic biopolymers- reinforced bioactive glass scaffolds with improved mechanical properties in wet state.** Materials Letters, p. 75-80, 2012.
- YAO, Q.; LI, W.; YU, S.; MA, L.; JIN, D.; BOCCACCINI, A.R. LIU, Y.**Multifunctional chitosan/polyvinyl pyrrolidone/45S5 Bioglass® scaffolds for MC3T3-E1-E1 cell stimulation and drug release.** Materials Science and Engineering C, v. 56, p. 473-480, 2015
- YUNOS, D.M.; BRETCANU, O.; BOCCACCINI, A.R. **Polymer-bioceramic composites for tissue engineering scaffolds.**Materials Science, v.43, n.13, p.4433-4442, 2008.
- ZABOROWSKA,M.;BODIN,A.;BACKDAHL,H.;POPP,J.; GOLDSTEIN,A.;
- GATENHOLM, P. **Micro-porous bacterial cellulose as a potential scaffold for bone regeneration,** ActaBiomaterialia, v. 6, p. 2540- 2547, 2010.

ZARIFAH, N.; LIM, W.; MATORI, K.; SIDEK, H.; WAHAB, Z.; ZAINUDDIN, N.; SALLEH, M.; FADILAH, B.; FAUZANA, A. **An elucidating study on physical and structural properties of 45S5 glass at different sintering temperatures.** *Journal of Non-Crystalline Solids*, v. 412, p. 24–29, 2015.

ZHAO C, TAN A, PASTORIN G, HO H. **Nanomaterial scaffolds for stem cell proliferation and differentiation in tissue engineering.** *Biotechnol. Adv.*, v. 31, p. 654–668, 2013.

ZHONG, Z.; QIN J.; MA, J. **Cellulose acetate/hydroxyapatite/chitosan coatings for improved corrosion resistance and bioactivity.** *Material Science and Engineering C*, v 49, p. 251–255, 2015.

ZHU, H., JIA, S., YANG, H., TANG, W., JIA, Y., TAN, Z., **Characterization of Bacteriostatic Sausage Casing: A Composite of Bacterial Cellulose Embedded with Polylysine.** *Food Science and Biotechnology*, v. 19, p. 1479-1484, 2010.

ZHU, Y.; KASKEL, S. **Comparison of the *in vitro* bioactivity and drug release property of mesoporous bioactive glasses (MBGs) and bioactive glasses (BGs) scaffolds.** *Microporous Mesoporous Materials*, p. 176-182, 2009.

ZIMMERMANN, K. A.; LEBLANC, J. M.; SHEETS, K. T.; FOX, R. W.; GATENHOL, M, P.

Biomimetic design of a bacterial cellulose/hydroxyapatite nanocomposite for bone healing applications. *Materials Science and Engineering: C*, v. 31, p. 43-49, 2011.